Journal of Medicinal Chemistry

Article

Cite This: J. Med. Chem. 2018, 61, 329−343

pubs.acs.org/jmc

A Stable Heroin Analogue That Can Serve as a Vaccine Hapten to Induce Antibodies That Block the Effects of Heroin and Its Metabolites in Rodents and That Cross-React Immunologically with Related Drugs of Abuse

Agnieszka Sulima,[†] Rashmi Jalah,[‡,§] Joshua F. G. Antoline,[†] Oscar B. Torres,[‡,§] Gregory H. Imler,[∥] Jeffrey R. Deschamps,[∥] Zoltan Beck,[‡,§] Carl R. Alving,[§] Arthur E. Jacobson,[†] Kenner C. Rice,*[,†] and Gary R. Matyas*[,§]

[†]Drug Design and Synthesis Section, Molecular Targets and Medications Discovery Branch, Intramural Research Program, National Institute on Drug Abuse and the National Institute on Alcohol Abuse and Alcoholism, National Institutes of Health, Department of Health and Human Services, 9800 Medical Center Drive, Bethesda, Maryland 20892-3373, United States

[‡]U.S. Military HIV Research Program, Henry M. Jackson Foundation for the Advancement of Military Medicine, 6720A Rockledge Drive, Bethesda, Maryland 20817, United States

[§]U.S. Military HIV Research Program, Walter Reed Army Institute of Research, 503 Robert Grant Avenue, Silver Spring, Maryland 20910, United States

[∥]Center for Biomolecular Science and Engineering, Naval Research Laboratory, Washington D.C. 20375, United States

Supporting Information

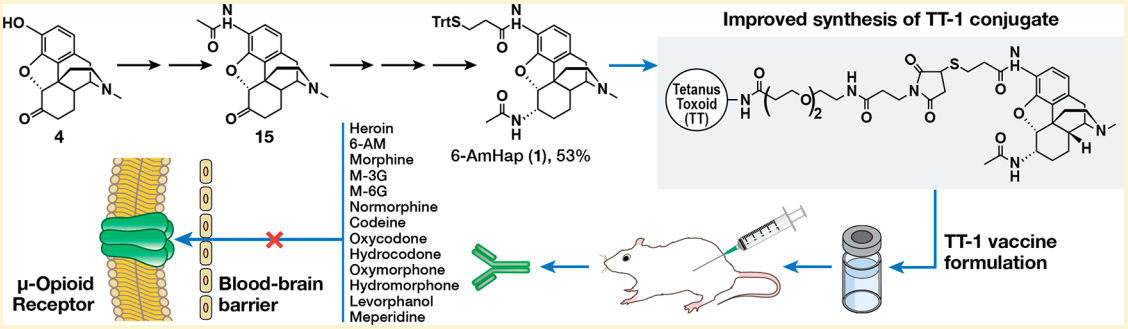

ABSTRACT: An improved synthesis of a haptenic heroin surrogate **1** (6-AmHap) is reported. The intermediate needed for the preparation of **1** was described in the route in the synthesis of **2** (DiAmHap). A scalable procedure was developed to install the C-3 amido group. Using the Boc protectng group in **18** allowed preparation of **1** in an overall yield of 53% from **4** and eliminated the necessity of preparing the diamide **13**. Hapten **1** was conjugated to tetanus toxoid and mixed with liposomes containing monophosphoryl lipid A as an adjuvant. The **1** vaccine induced high anti-**1** IgG levels that reduced heroin-induced antinociception and locomotive behavioral changes following repeated subcutaneous and intravenous heroin challenges in mice and rats. Vaccinated mice had reduced heroin-induced hyperlocomotion following a 50 mg/kg heroin challenge. The **1** vaccine-induced antibodies bound to heroin and other abused opioids, including hydrocodone, oxycodone, hydromorphone, oxymorphone, and codeine.

INTRODUCTION

The abuse of opioids, which include heroin and fentanyl, is a growing problem in the United States that is partly responsible for the recently declared National Emergency for Opioid crisis. Between 2007 and 2015, the number of past year heroin users increased from 373000[1] to 828000,[2] of which 591000 were classified as heroin dependent.[2] Between 2006 and 2015, the number of heroin-related deaths increased over 600%, from 2088 to 12989.[3] Our ability to prevent the spread of heroin abuse and aid heroin addicts is handicapped by the lack of sufficient treatment modalities for heroin addiction. Most pharmacological treatments for opioid abuse involve opioid management therapy (OMT) regulated administration of opioid medications with fewer side effects, such as methadone and, more recently, buprenorphine alone or in conjunction with naloxone.[4] While effective, OMT program adherence rates vary substantially, and the relapse rates for heroin users who complete or discontinue OMT is higher than for those who abuse other opioids.[5] In addition, treatment access and

Received: September 29, 2017
Published: December 13, 2017

DOI: 10.1021/acs.jmedchem.7b01427
J. Med. Chem. 2018, 61, 329−343

drug diversion are problems for opioid-based treatment options.[6] If the heroin problem is to be solved, many different types of treatments and medications will be needed to meet the needs of the individual addict.

A promising addition to traditional drug-based treatments is immunopharmacotherapy, in which antibodies bind to a substance of abuse and prevent the substance from penetrating the blood−brain (bb) barrier and subsequently act on the opioid receptors in the brain.[7−9] Vaccine-induced antibodies (active immunization) or monoclonal antibodies (passive immunotherapy) "kinetically sequester" opioids from the peripheral circulation and thereby recompartmentalizing them in the blood instead of the brain. It also has been suggested that this sequestration shifts the opioid concentration gradient in the bb barrier, which favor the efflux of the opioid from the brain to the blood.[10] Because opioids are too small to be recognized by the immune system, an opioid-based hapten can be conjugated to a carrier protein and used as a vaccine to induce antibodies that can recognize the hapten as well as heroin and/or other opioids. A major difficulty in attempting to prevent heroin from reaching brain opioid receptors is due to the fact that heroin is a prodrug with a very short half-life (2−6 min).[11] Its initial major metabolite, 6-acetylmorphine (6-AM), is also readily transported to the brain and also has high affinity for the μ-opioid receptor.[12] For a heroin vaccine to be effective, it would need to generate antibodies that target both heroin and its metabolites. Two different heroin vaccine strategies based on hapten design have been reported. The first is haptens based on metabolically stable compounds like morphine that induce antibodies that bind to morphine and 6-AM but have a more limited ability to cross-react with heroin.[12−19] A stable version of this type of hapten, wherein the C-6 ester is changed to amide, has been reported.[14] The second is haptens that are based on metabolically unstable heroin, which evoke polyclonal antibodies that contain separate populations of antibodies that react separately with morphine, 6-AM, or heroin.[20−23] The chemical instability of this type of hapten is due to the presence of labile ester groups at the C-3 and C-6 positions. However, because this type of hapten is unstable, it is expected to have a limited shelf life because it can degrade during vaccine manufacturing and storage. Both of these two strategies induce antibodies that had limited ability to cross-react with other currently abused opioids like codeine[14,16,22] and oxycodone.[15,22] To address the above problems and produce a more effective heroin-focused vaccine with broader antiopioid specificities, we have developed a novel third type of hapten, **1** (6-AmHap, *N*-((7*S*,7a*R*,12b*S*)-7-acetamido-3-methyl- 2,3,4,4a,5,6,7,7a-octahydro-1*H*-4,12-methanobenzofuro-[3,2-*e*]isoquinolin-9-yl)-3-(tritylthio)propanamide), which is a stable hapten that incorporates the hydrolytically stable amide functionality into the 4,5-epoxymorphinan core and a 3-(tritylthio)propanamide linker for bioconjugation at the C-3 position on the aromatic ring (**1**, Figure 1). Although our previous studies indicated that **2** (DiAmHap)[24] and **3** (MorHap)[14,25] were promising vaccine candidates, we report here that **1** is a more effective hapten against not only heroin and its metabolites but also abused prescription narcotics like hydromorphone and oxycodone.[26] Hapten **1** is compared in this study to **3**, a morphine-based hapten that was efficacious against heroin challenge.[14]

Because multigram quantities of hapten **1** were needed to run our in vitro and in vivo studies, to conduct current Good Laboratory Practices (cGLP) toxicology studies, and to obtain sufficient supplies for eventual human clinical studies under current Good Manufacturing Practices (cGMP) regulations, we needed a multigram quantity of material and the most facile method for obtaining that material that we could devise. We sought a scalable and higher yielding synthesis.

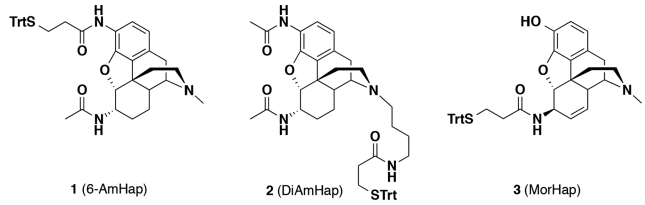

Figure 1. Structure of heroin haptens **1**, **2**, and **3**.

RESULTS AND DISCUSSION

Chemistry. The initial synthesis of **1** utilized **12** (previously prepared,[24] Scheme 1), which was also an intermediate to **2**. Hapten **1** was obtained from compound **12** via TBTU coupling with 3-(tritylthio)propionic acid in 76% yield, with an overall yield of 12% from hydromorphone **4** (Scheme 1). Compound **2** had been obtained (Scheme 1) via a sequential *N*-acylation, *N*-demethylation, followed by *N*-alkylation in 7% overall yield from hydromorphone **4** (Scheme 1). The reported demethylation procedure was attempted with compound **13**[24,27] to obtain **14**, and it proved somewhat problematic. Thus, a demethylation protocol was applied[28] using ethyl chloroformate/trimethylsilyl iodide, which gave **14** in 65% yield. Compound **14** could be converted to **2** in 76% via the established procedure (Scheme 1).

While the synthesis in Scheme 1 was effective at delivering screening quantities of haptens **1** and **2**, the material throughput left much to be desired. It was important to explore alternate routes in order to obtain **1** in higher yield and fewer steps for our in vitro and in vivo studies and to aid the adaptation of the synthesis of the hapten for compliance with the FDA's cGMP regulations. We began with an investigation of the direct C(3)−N bond formation via aryl amidation that we envisioned would dramatically shorten the synthesis going directly from triflate **5** to acetamide **15** (Scheme 2).

Since the seminal work by Migita on the coupling of aryl bromides and amino stannanes in 1984,[29] palladium catalyzed C−N cross couplings have grown in both scope and utility.[30] The pioneering work by the Buchwald group has led to the development of specialized biaryl phosphine ligands and catalyst activation protocols that have been shown to be effective for both aryl amination and amidation on electron-rich and sterically hindered systems. On the basis of the triflate reduction in the original synthetic route (Scheme 1, compound **5** to **6**), we knew that it was possible for palladium to insert into the aryl C−O bond with triphenylphosphine as a ligand, but it remained to be seen if that was possible with the bulky biaryl phosphine ligands used to promote C−N coupling.

An initial screen was conducted to probe the viability of the reaction, employing readily available catalysts and ligands. Both the palladium-mediated Buchwald−Hartwig type coupling and the copper-catalyzed Goldberg coupling were screened. The Goldberg coupling proved to be ineffective, which was not surprising given the generally lack of reactivity of aryl sulfonates to copper-catalyzed couplings.[31] Gratifyingly, trace quantities of the desired product were detected via GC/MS

DOI: 10.1021/acs.jmedchem.7b01427
J. Med. Chem. 2018, 61, 329−343

Scheme 1. Initial Synthesis of 1 and 2

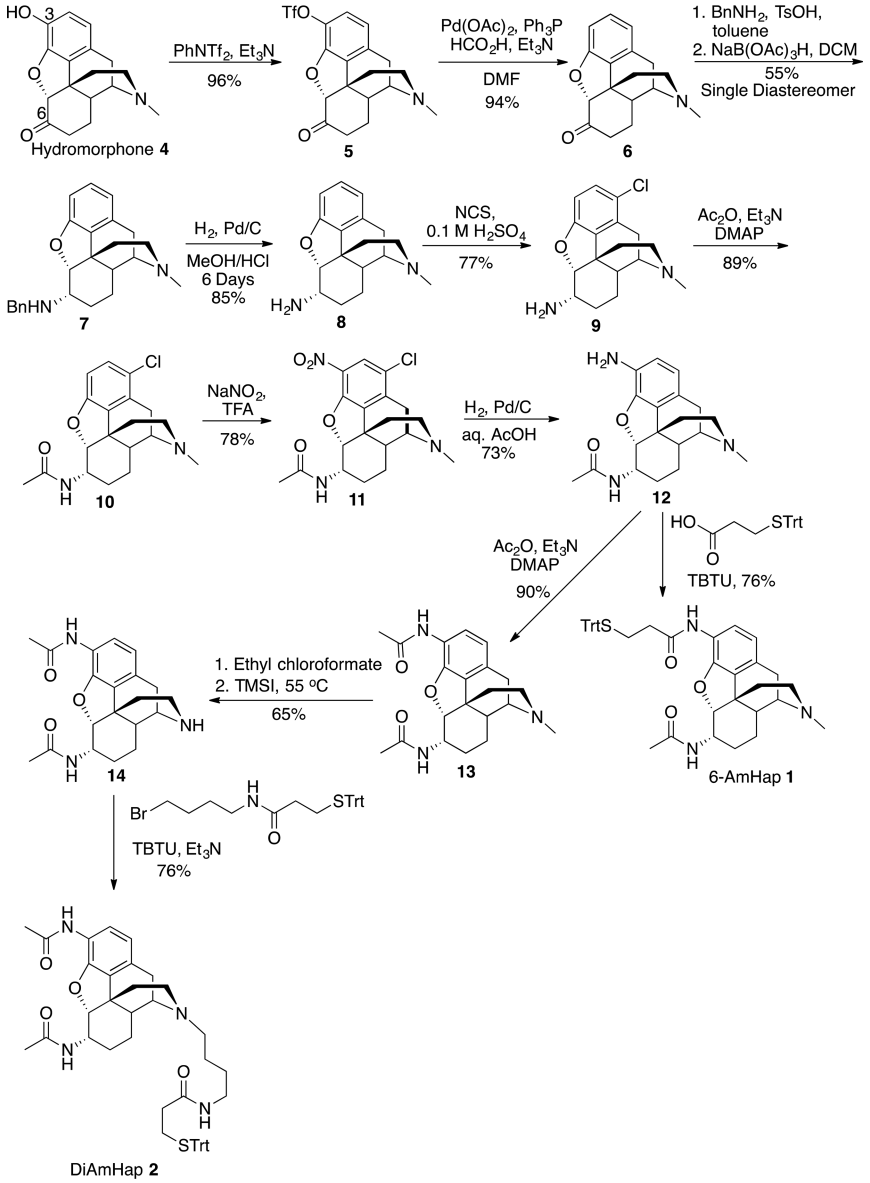

Scheme 2. Envisioned Improvement of the Synthesis of Haptens 1 and 2

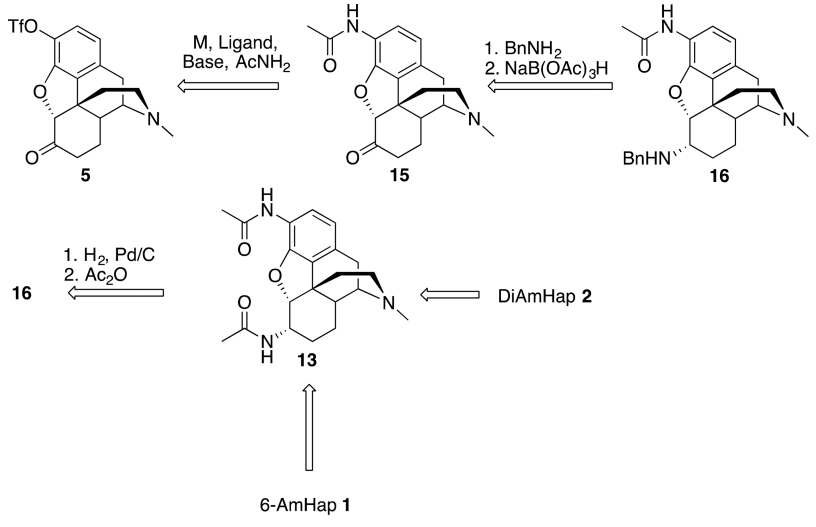

DOI: 10.1021/acs.jmedchem.7b01427
J. Med. Chem. 2018, 61, 329−343

Table 1. Aryl Amidation with Third-Generation Palladacycle Catalyst

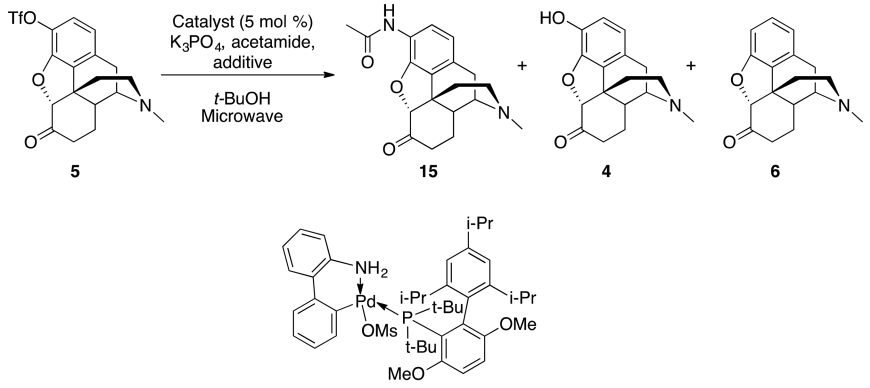

Catalyst: *tert*-Butyl BrettPhos palladacycle

entry	scale (mmol)	additive	time (min)	temp (°C)	result (GC)
1	0.28	none	100	110	**15** (82%), trace[a] **4**
2	2.8	none	240	110	**15** (37%), trace[a] **4**, **6**
3	0.23	4 Å MS	270	120	**15** (21%), trace[a] **4**, **6**
4	3.3	H_2O (1 equiv)	120	110	**15** (73%), trace[a] **6**
5	19.16	H_2O (1.15 equiv)	240	90 (conventional heating)	**15** (88%)

[a]The ratio of the GC peak integration of listed compounds to **15** is ≤0.05.

using the $Pd_2(dba)_3$/XantPhos catalyst system, prompting a more systematic investigation. A range of variables was explored in the Buchwald-type coupling, including XantPhos, XPhos, BrettPhos, and CyJohnPhos phosphine ligands and catalyst/base/solvent combinations ($Pd(dba)_3$, $Pd(OAc)_2$, Cs_2CO_3, K_3PO_4, K_2CO_3, *t*BuOH, toluene, dioxane) that have been historically successful for aryl amidation of sulfonates.[30] While we observed a rapid consumption of the starting material under some of the applied conditions, the desired product **15** was accompanied by significant amounts of phenolic byproducts **4** and **6**.

Bruno and Buchwald recently reported a third generation of the palladacycle catalysts, incorporating extremely bulky di-*tert*-butylphosphino ligands, capable of amidation of electron rich, *ortho*-substituted aryl chlorides.[32] These *tert*-butyl-substituted phosphine catalysts are more efficient at promoting the reductive elimination step of the catalytic cycle, which is the most difficult step when coupling electron-rich substrates and amide nucleophiles.[33] We employed the *tert*-butyl BrettPhos palladacycle precatalyst (Table 1) in the reaction of **5** with acetamide under microwave heating conditions. The new precatalyst dramatically outperformed the previously screened ligand/catalyst systems, giving the desired amide in less time and higher yield on a 0.2−0.3 mmol scale, with almost no detectable phenolic byproducts (Table 1, entry 1). When scaling the reaction up by an order of magnitude, the reaction time increased and the yield dropped sharply (Table 1, entry 2). Importantly, only trace amounts of **4** and **6** were detected when running the reaction on a larger scale. After much deliberation, we thought it is possible that the presence of water may be affecting the amount of product formed, and indeed, water was found to have a significant impact on the conversion of **5** to **15** as demonstrated by examples 3 and 4 (Table 1). The addition of an equivalent of water increased the yield of the multigram scale reactions under microwave and conventional heating to 73% and 88%, respectively, without significant formation of phenolic byproducts (Table 1, entries 4 and 5).

Having improved the aryl amidation, we considered the next step, the installation of the C-6 acetamide. The C-3 acetamide moiety of **15** was found to be unstable under the original tosic acid-catalyzed reductive amination conditions that were successful on deoxyhydromorphone **6**. Instead, the reductive amination was performed under basic conditions using the procedure developed by Hudson and Sweeney[34] to give amine **16** contaminated with benzylamine (Scheme 3). Hydrogenolysis of the impure mixture **16** gave crude **17**, which was acylated to give **13** in 67% yield from **6**. The C-6 stereochemistry was confirmed by comparison with samples of **13** prepared by the original route (Scheme 1). Demethylation

Scheme 3. Synthesis of 1 from 15

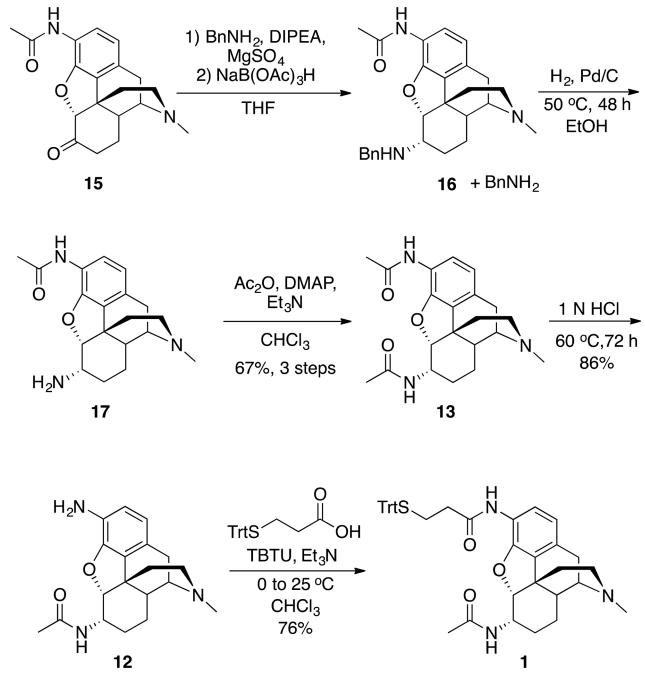

DOI: 10.1021/acs.jmedchem.7b01427
J. Med. Chem. 2018, 61, 329−343

Scheme 4. Scalable Synthesis of 1

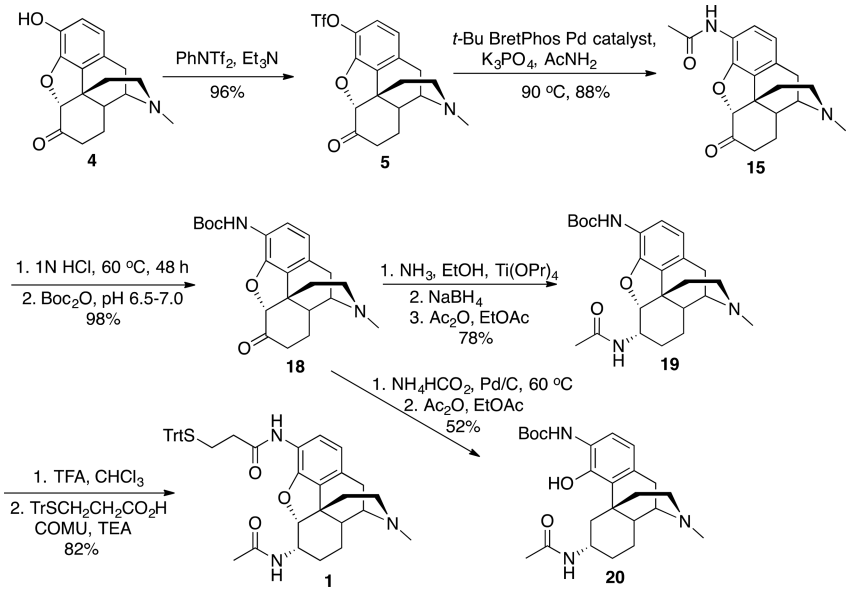

with ethyl chloroformate/TMSI (Scheme 1) afforded compound **14**, which could be elaborated by the previously established procedure to give **2** in 7 steps from hydromorphone in 23% overall yield.

Conversion of **13** to **1** (Scheme 3) required the selective hydrolysis of the aryl C-3 acetamide in the presence of the aliphatic C-6 acetamide. This was accomplished by the carefully monitored heating of **13** in 1 N hydrochloric acid at 60 °C for 72 h. Higher concentrations of acid, longer reaction times, or higher temperatures increased the quantity of the double hydrolysis product. Coupling of **12** with 3-(tritylthio)propionic acid with TBTU gave **1** in 76%, a 31% overall yield from hydromorphone. Although this was a considerable improvement over the earlier work, we wanted to avoid the somewhat problematic, selective hydrolysis of diacetamide **13** (Scheme 3). Thus, a new route was devised using a *tert*-butyloxycarbonyl (Boc) protected intermediate.

Hydrolysis of the C-3 acetamide **15** and the introduction of a Boc group provided more of the desired regioselectivity and control in deprotection of compound **19** at the later stage of the synthesis (Scheme 4). The Boc protected intermediate **18** was prepared in a one-pot procedure via acidic hydrolysis of **15** followed by treatment with Boc anhydride at pH < 7. Because the previously applied reductive amination sequence (Scheme 3) involved debenzylation that was sluggish (48 h at 50 °C) (Scheme 3), we tried a different approach. We used a titanium(IV) isopropoxide-assisted reductive amination of **18** with ammonia in ethanol, followed by in situ sodium borohydride reduction[35] (Scheme 4) to give an amine intermediate. The amine intermediate was subsequently reacted with acetic anhydride in anhydrous ethyl acetate[36] to yield **19** (Scheme 4). Single-crystal X-ray analysis of **19** confirmed the absolute stereochemistry of the C-6 asymmetric center (Figure 2). Interestingly, if the reductive amination of **18** was carried out in the presence of palladium catalyst and ammonium formate at elevated temperature,[37] the oxide bridge underwent ring-opening to form the unwanted phenol intermediate **20** (Scheme 4). The structure of **20** was confirmed by single-crystal X-ray analysis of its hydrochloride salt (Figure 3). Finally, hydrolysis of the Boc protecting group

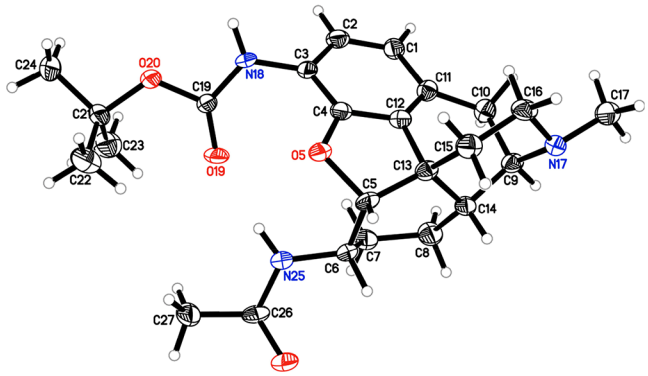

Figure 2. X-ray crystallographic structure of diamide **19**. Displacement ellipsoids are shown at the 50% level.

of **19** (Scheme 4) in the presence of trifluoroacetic acid went smoothly to yield the intermediate that was successfully

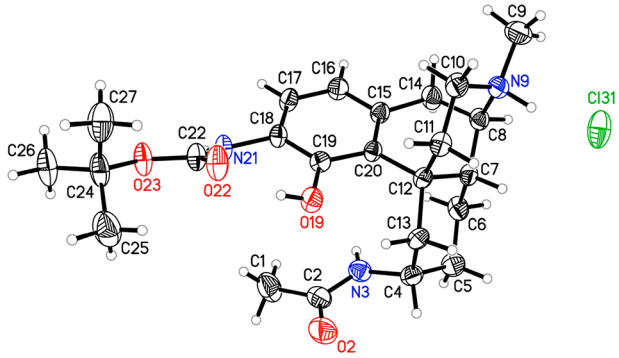

Figure 3. X-ray crystallographic structure of oxide ring-opened product **20**. Displacement ellipsoids are shown at the 50% level.

coupled to 3-(tritylthio)propionic acid to provide the target hapten **1** in 53% overall yield from hydromorphone **4**, an improvement over the original route that gave **1** in a 12% yield from **4**.

DOI: 10.1021/acs.jmedchem.7b01427
J. Med. Chem. 2018, 61, 329−343

Biology. Hapten **1** was compared with the previously reported morphine-like hapten, **3**.[14,18] Conjugation of both **1** and **3** to the tetanus toxoid (TT) carrier protein yielded 34 (31−37) haptens attached per TT molecule as measured by MALDI-TOF mass spectrometry (Supporting Information, Figure S1). The protein yield of the conjugation was ≥90% for both TT−**1** and TT−**3** bioconjugates with minimal protein precipitation. Both conjugates had similar sizes, and none of the conjugates formed any high molecular weight protein aggregates as confirmed by their patterns on nonreducing SDS PAGE and Blue Native PAGE gels (Supporting Information, Figure S2).

TT−**1** and TT−**3** conjugate vaccines were mixed with Army Liposome Formulation (ALF)[38] as an adjuvant and subsequently tested and compared in mice. The study design for the testing of TT−**1** and TT−**3** vaccines in mice is illustrated in Supporting Information, Figure S3. Both vaccine formulations induced similar high antihapten antibody titers after each immunization (Figure 4, p = ns). Following three

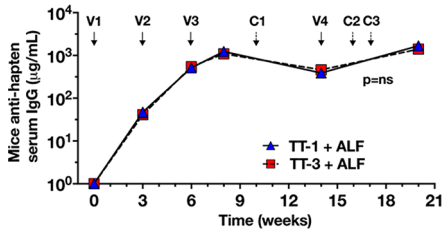

Figure 4. Time course of TT−**1** and TT−**3** vaccine induced heroin hapten specific serum IgG antibody levels (μg/mL) in mice. Vaccine administration (V1−V4) and heroin challenges (C1, SC route; C2, IV route; C3, IV route) are indicated by arrows.

vaccinations, high mean IgG levels of 1.1 and 1.2 mg/mL were induced for TT−**3** and TT−**1**, respectively. Despite a 2−3-fold decline during the 6-week period from week 8 to week 14, high levels of hapten antibodies ranging from 0.2 to 0.8 mg/mL were maintained. Following immunization at week 14, the antihapten IgG levels were restored with mean levels of 1.4 and 1.7 mg/mL for TT−**3** and TT−**1**, respectively, at 6 weeks after the immunization (Figure 4). There were no significant differences (p = ns) between the TT-specific carrier antibody responses as well, which were 72.6 ± 24.2 and 99.7 ± 19.6 μg/mL at week 8 for TT−**1** and TT−**3**, respectively (Supporting Information, Figure S4A).

Both TT−**1** and TT−**3** vaccine formulations provided significant inhibition of heroin-induced antinociception in the tail flick assay with a mean %MPE of 7−29% following three heroin challenges (C1, C2, and C3): subcutaneous (SC) at week 10 (C1) and repeated intravenous (IV) heroin challenges at weeks 16 (C2) and 17 (C3). The unvaccinated control mice had a mean %MPE of 82−90% (Figure 5, top panel). Heroin administration increased locomotion above baseline in the control mice, resulting in increased levels in the total distance moved (Figure 5, bottom panel). In comparison, mice from both vaccinated groups significantly suppressed this heroin-induced hyperlocomotion upon heroin challenge as compared to the control unvaccinated animals. There were no significant differences between the animals receiving TT−**1** and TT−**3** on their ability to block heroin effects in both assays (p = ns). These results indicated that both vaccines provided similar and potent protection upon heroin challenge in mice.

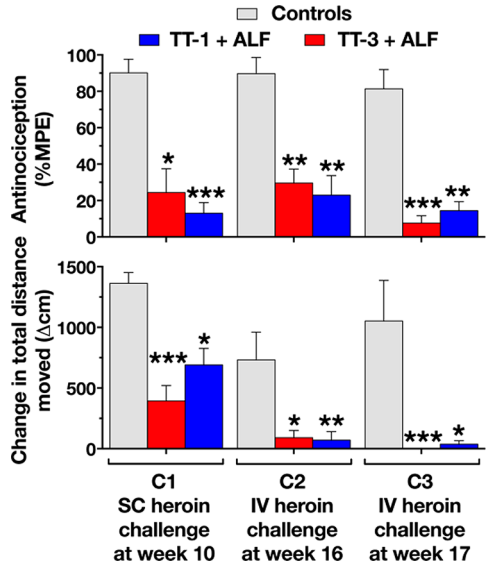

Figure 5. TT−**1** and TT−**3** vaccine efficacy upon repeated heroin challenges in the tail flick antinociception assay (top panel) and the locomotion assay (bottom panel) in mice. Unvaccinated control mice and mice immunized with either TT−**1** + ALF or TT−**3** + ALF were challenged with SC heroin (C1, 1 mg/kg) and IV heroin (C2 and C3, 0.5 mg/kg). For the tail flick assay, antinociception is expressed as percent of maximum possible effect (%MPE). For the locomotion assay, the values are expressed as differences between the post minus the pre heroin values for the total distance traveled. All values represent mean ± SEM of 10 mice per group. Asterisks indicate significant differences in the vaccine groups as compared to the corresponding unvaccinated control mice for each heroin challenge (*, $p < 0.05$; **, $p < 0.01$; ***, $p < 0.001$) using one-way ANOVA; Kruskal−Wallis test with Dunn's correction for multiple comparisons. The mean ± SEM baseline value for all groups for total distance moved in 5 min before heroin injection (pre heroin) was 1107 ± 46 cm and for mean velocity was 3.7 ± 0.2 cm/s.

To test the efficacy of the TT−**1** vaccine at high heroin dose (i.e., 50-fold greater than Figure 5), mice were challenged with 50 mg/kg SC heroin following three vaccinations with TT−**1** with ALFA adjuvant (ALF adsorbed to aluminum hydroxide (AH)). The vaccine formulation generated high **1** specific titers of approximately 1 mg/mL at week 8 (data not shown) and significantly reduced the heroin-induced hyperlocomotion following heroin challenge. The control animals challenged with heroin moved ∼8-fold farther than their preheroin challenge baseline levels, and the TT−**1** vaccinated mice had their locomotion significantly dampen by approximately 1.5-fold compared to control animals. The effect was more prominent between 10 and 25 min post heroin injection (Figure 6).

We further tested the efficacy of TT−**1** mixed with ALF as an adjuvant in rats (Supporting Information, Figure S5) following a similar vaccination schedule as with mice (Supporting Information, Figure S3). Vaccination of rats with TT−**1** induced ∼10-fold higher antibody titers than that of mice with very high mean peak IgG levels of approximately 12 mg/mL at week 8 and were maintained for 13 weeks after the last booster immunization (Figure 7). The TT-specific carrier antibody levels were also approximately 40-fold higher in rats (3.1 ± 0.3 mg/mL) as compared to mice (Supporting Information, Figure S4B).

DOI: 10.1021/acs.jmedchem.7b01427
J. Med. Chem. 2018, 61, 329−343

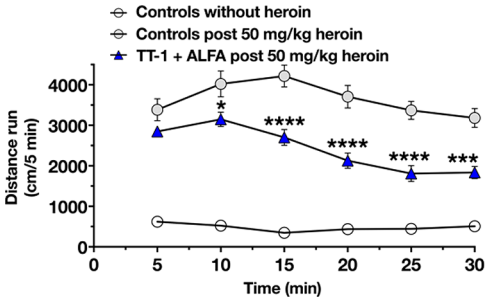

Figure 6. TT−**1** vaccine efficacy following high dose heroin challenge in mice. Unvaccinated control mice and mice immunized with TT−**1** with ALFA as adjuvant (n = 10 mice per group) were challenged with high dose of 50 mg/kg SC heroin, and their locomotion was monitored for 30 min before and after challenge. The total distance traveled per 5 min segments (cm, mean ± SEM) over a period of 30 min is shown. Asterisks indicate significant differences between the control and TT−**1** vaccinated groups at each time point after heroin injection (*, $p < 0.05$; ***, $p < 0.001$; ****, $p < 0.0001$) using two-way ANOVA with Sidak's multiple comparisons test.

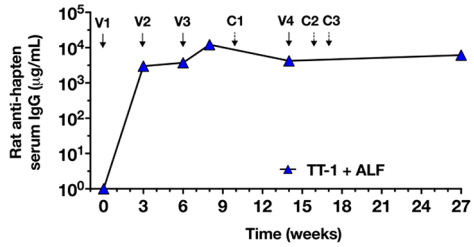

Figure 7. Time course of TT−**1** vaccine induced heroin hapten specific serum IgG antibody levels (μg/mL) in rats. Vaccine administration (V1−V4) and heroin challenges (C1−C3) are indicated by arrows.

Rats vaccinated with formulations containing TT−**1** with ALF adjuvant demonstrated significantly lower mean %MPE of 27−48% in the tail immersion assay as compared to the unimmunized controls with 96−100% %MPE following SC (at weeks 10 and 17) and IV (at week 16) heroin challenges (Figure 8, top panel). In the thermal place preference test (TPPT), the control rats moved randomly between the two plates after heroin injection, with several of them not moving from the hot plate for more than 30 s and were removed to avoid burns. In contrast, the TT−**1** vaccinated rats spent more time on the plate at 25 °C with several of them staying there continuously. Thus, they spent significantly lower % of the total assay time on the hot plate in the TPPT assay as compared to the control animals (Figure 8, bottom panel). Overall, the TT−**1** vaccines gave high titer antibodies and potent protection from heroin challenge in rats.

Competition ELISA studies were conducted to assess the binding specificities of the hapten-induced antibodies to heroin, its metabolites, other opioids, and opioid abuse therapeutic drugs (Table 2, Supporting Information, Tables S1 and S2). Low IC_{50} values correspond to high affinity hapten-induced antibodies to the target drug. In general, competition ELISA IC_{50} values tend to numerically overestimate the actual K_d values of the antibodies by 10^3-fold.[20] Thus, the IC_{50} values measured by competition ELISA in the μM range are expected to correspond to K_d values in the nM range.[39] The structures of the drugs, which were used in the competition ELISA, are provided in Supporting Information,

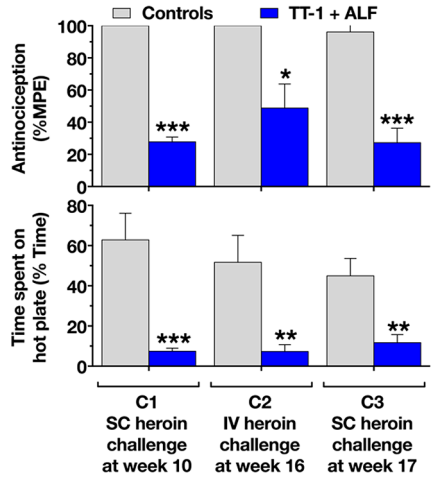

Figure 8. TT−**1** vaccine efficacy upon repeated heroin challenges in the tail immersion antinociception assay (top panel) and the thermal place preference, two-temperature zone choice test (TPPT) (bottom panel) in rats. Unvaccinated control rats and rats immunized with TT−**1** + ALF were challenged with SC heroin (C1, 1 mg/kg), IV heroin (C2, 0.5 mg/kg), and SC heroin (C3, 1 mg/kg). For the tail immersion assay, antinociception is expressed as percent of maximum possible effect (%MPE). For TPPT, the values are expressed as % total time spent on the hot plate. Several control rats (n = 4, 2, and 1 at 1st (C1) and 2nd (C2) challenge, respectively) were removed to avoid burns after reaching the continuous 30 s hot side cutoff in TPPT and were scored as 100% on the hot side. All values represent mean ± SEM of 8 rats per group. Asterisks indicate significant differences in the vaccine groups as compared to the corresponding unvaccinated control rats for each heroin challenge (*, $p < 0.05$; **, $p < 0.01$; ***, $p < 0.001$) using Mann−Whitney nonparametric t test.

Figure S6. TT−**1**-induced antibodies from mice had significantly lower IC_{50}s than TT−**3**-induced antibodies to heroin and its metabolites, 6-AM, morphine, morphine-3-β-glucuronide (M-3G), and morphine-6-β-glucuronide (M-6G). However, the IC_{50}s to normorphine were significantly lower for **3** (Supporting Information, Figure S7). None of the hapten-induced antibodies bound the drugs used for opioid abuse therapy, i.e., methadone, buprenorphine, and naltrexone (IC_{50} > 1000) or to naloxone, which is the overdose rescue therapy (Supporting Information, Figure S8). In addition, unlike **3**-induced antibodies, **1**-induced antibodies cross-reacted with significantly lower IC_{50}s to multiple other abused prescription opioid drugs like codeine, oxycodone, hydrocodone, and hydromorphone (Supporting Information, Figure S9). Antibodies induced by both haptens had similar strong binding to oxymorphone and levorphanol. None of the hapten-induced antibodies bound tramadol, fentanyl, sufentanil, and nalbuphine and poorly to meperidine, which are structurally unrelated opioids to heroin (Supporting Information, Figure S9). There was no binding to the non-narcotic analgesics like acetylsalicylic acid, ibuprofen, and acetaminophen (Supporting Information, Figure S10). Antibodies to both haptens did not bind the human endogenous opioid peptides β-endorphin and [Leu5]-enkephalin (Supporting Information, Figure S11). **1** antibodies from rats (Table 2 and Supporting Information, Table S2) exhibited similar binding affinity trends as mice (Supporting Information, Table S1) to heroin and its metabolites (Supporting Information, Figure S12), and other abused prescription opioid drugs (Supporting Information, Figure S13), but not to opioid abuse therapeutics (Supporting

DOI: 10.1021/acs.jmedchem.7b01427
J. Med. Chem. 2018, 61, 329−343

Table 2. Inhibition Concentration 50% (IC_{50}; μM) for Various Opioids Measured Using Competition ELISA[a]

	mice antibody IC_{50}		rat antibody IC_{50}
	TT-3 + ALF	TT-1 + ALF[b]	TT-1 + ALF[b]
Heroin and Its Metabolites			
heroin	>1000	1.27 ± 0.3***	3.0 ± 0.6***
6-AM	104.4 ± 14.8	3.72 ± 0.7***	1.5 ± 0.6***
morphine	24.3 ± 4.5	2.36 ± 0.6***	7.1 ± 2.7*
M-3G	>1000	28.0 ± 11.4***	35.5 ± 14.7***
M-6G	411.0 ± 94.4	25.0 ± 12.1**	104.4 ± 46.6
normorphine	19.7 ± 2.5	112.43 ± 22.3	192.9 ± 57.1
Drugs Used for Opioid Abuse Therapy			
methadone	>1000	>1000	>1000
buprenorphine	>1000	>1000	>1000
naloxone	>1000	>1000	>1000
naltrexone	>1000	>1000	>1000
Other Abused Prescription Opioid Drugs			
codeine	>1000	3.80 ± 1.3***	17.2 ± 5.4***
oxycodone	>1000	534.6 ± 79.5***	144.6 ± 60.6***
hydrocodone	>1000	5.1 ± 1.5***	14.7 ± 2.7***
oxymorphone	110.4 ± 24.5	125.5 ± 28.6	217.1 ± 94.8
hydromorphone	59.7 ± 19.2	3.6 ± 0.8*	23.8 ± 8.8
levorphanol	9.7 ± 4.8	3.4 ± 0.9	53.6 ± 28.1
meperidine	>1000	523.9 ± 143.3*	>1000
tramadol	>1000	>1000	>1000
fentanyl	>1000	>1000	>1000
sufentanil	>1000	>1000	>1000
nalbuphine	>1000	>1000	>1000

[a]Values denote IC_{50} for the indicated drugs (μM; mean ± SEM) measured using competition ELISA from individual animal sera for each group using triplicate measurements. IC_{50} was defined as the drug concentration that produced 50% inhibition of maximal antibody and hapten binding as calculated from normalized competition curves using log(inhibitor) vs normalized response-variable slope regression. [b]Asterisks indicate groups with significantly lower IC_{50} (higher affinity) as compared to the mice group immunized with TT-3 (***, $p < 0.0001$; **, $p < 0.001$; *, $p < 0.01$) using multiple t test with Holm−Šídák correction.

Information, Figure S14), non-narcotic analgesics (Supporting Information, Figure S15), and endogenous opioid peptides (Supporting Information, Figure S16). Overall, the binding specificity of antibodies induced by the **1** vaccine strongly suggest that the **1** vaccine is not only a vaccine that induces antibodies that block the biological activity of heroin and its metabolites but also a vaccine that induces antibodies that can potentially block the activity of morphinan-based opioids.

The development of a successful heroin vaccine requires the induction of high titer and durable antibodies with high affinity to heroin and its metabolites. Here we have described TT−**1**, a novel heroin vaccine that utilizes a unique hydrolytically stable heroin-like hapten, **1**, conjugated at C-3 position to TT. TT is the antigen in the licensed tetanus vaccine and also has been widely used as a carrier protein for conjugate vaccines.[14,40,41] The TT−**1** was formulated with ALF or ALFA, which are potent and generic adjuvants that, based on multiple clinical trials, should be safe and effective.[38,40,42−46] The vaccine elicited high antibody levels and protective immunity from repeated SC and IV heroin challenges in mice and rats. The IV route was chosen as it closely mimics injection drug abuse in humans. In addition, the vaccine induced antibodies that cross-reacted with heroin and sequentially produced active metabolites: 6-AM, morphine and M-6G as assessed by competition ELISA. Comparison of the TT−**1** and TT−**3** vaccines revealed that there were no significant differences in antibody levels and efficacy from heroin challenge between the two vaccines. In general, the **1**-induced antibodies had a 10−20-fold lower IC_{50} in the competition ELISA than the **3**-induced antibodies. This suggests that TT−**1** vaccination should be more efficacious than TT−**3** immunization. Apparently, there is a threshold combination of antibody titer and affinity that is surpassed by immunization with vaccines containing **1** or **3**. This threshold may be related to the heroin dose used to challenge. Presumably, the antibody level and affinity must be sufficient to bind most of the heroin challenge dose. Bremer et al. have reported that their HerHap-based heroin vaccine protected up to 10 mg/kg of heroin administered by the SC route.[20,21] The threshold level of the **1** or **3** vaccines has not been tested. However, TT−**1** vaccinated mice challenged with 50 mg/kg of heroin by the SC route had a 1.5-fold reduction in the distance traveled when compared to the heroin challenged unvaccinated control animals (Figure 6). This indicates that even at this extremely high dose of heroin, the TT−**1** vaccine demonstrated partial efficacy, which may be sufficient to protect against heroin overdose. Approximately 50 mg (12−180 mg) of heroin has been reported to cause overdose in naïve humans.[47] On a weight basis, assuming a 70 kg human, this corresponds to about 0.72 mg/kg heroin. In this study, we had nearly complete protection from 1 mg/kg heroin, which would be expected to be lethal in humans. From a mathematical prospective, the amount of antibody circulating in the blood of a rat should be easily overcome by a 0.5 mg/kg dose of heroin, which is approximately 4-fold more heroin than antibody on a molar basis. This assumes the plasma volume of a 0.4 kg rat is ∼17 mL[48] and the antibody concentration is 1 mg/mL. The efficacy of the vaccine observed above and that reported by others[20,21] indicates that there are other

DOI: 10.1021/acs.jmedchem.7b01427
J. Med. Chem. 2018, 61, 329−343

nonquantifiable reserves of antibody, such as on the surface of B cells and plasma cells, that are not assessed by conventional ELISA on sera. In addition, the heroin may be dispersed throughout the body, thereby diluting the effective concentration in the blood. Regardless of the mechanism, animals vaccinated with TT−**1** were protected from a 0.5−1 mg/kg dose of heroin and mice vaccinated with the TT−**1** vaccine had partial efficacy against 50 mg/kg heroin, suggesting that the vaccine could prevent overdose of high doses of heroin in humans that are typically used by heroin addicts.

Depending on the hapten structure and linker attachment site, different faces of heroin/morphine molecule are presented to the immune system, resulting in variable reactivity of induced antibodies.[18] Morphine-like haptens have been coupled at the C-6 position using various coupling strategies by several groups.[13−19] This strategy has induced antibodies binding mainly to 6-AM and morphine with little or no affinity to heroin. The good efficacy of these vaccines in animal models may be due to the rapid degradation of heroin to 6-AM in the blood following injection. Despite rapid conversion to 6-AM, low levels of heroin were detected in the brain a few minutes after injection.[19,49] Thus, it is highly desirable that a heroin vaccine elicits high affinity antibodies to heroin, 6-AM, and morphine to completely sequester the drug in blood. Another strategy is the use of immunochemically "dynamic" vaccine that generates multiple haptens in situ and thus allows simultaneous presentation of relevant heroin metabolites to the immune system.[22] For example, a vaccine containing a "dynamic" heroin-like hapten, HerHap, conjugated at the bridge nitrogen atom elicited binding to heroin, 6-AM, and morphine due to degradation by deacetylation at the C-3 and C-6 position prior to or after immunization.[20−23] However, in our opinion, use of such a hapten would not be optimal due to its inherent instability because the half-life of acetyl group at the C-3 position of heroin was reported to be approximately a month at pH 7.4 at 4 °C.[11] This is expected to result in a short shelf life of HerHap bioconjugate as a vialed drug product. The TT−**1** vaccine described here is a better candidate that utilizes a unique stable C-3 linked heroin hapten with a hydrolytically stable amide by replacing the C-6 position acetyl group. The TT−**1** vaccine was able to abrogate heroin effects by the induction of antibodies with significantly higher affinities to heroin and all its metabolites as compared to morphine haptens.

The broad cross-reactivities of the antibodies induced by the TT−**1** vaccine suggests that it may also induce protective efficacy against other abused prescription opioids. The hapten **1**-induced antibodies were cross-reactive with high affinities to several other abused prescription opioids like hydromorphone, hydrocodone, codeine, oxymorphone, and oxycodone. Hapten **1** presented a face consisting of the bridgehead nitrogen, aliphatic ring, and the C-6 amide, corresponding to the C-6 hydroxyl in morphine (Supporting Information, Figure S17). Presumably, the portion of the antibody recognizing the C-6 position was promiscuous, accommodating amide, acetyl, ketone, and hydroxyl groups at this site (Table 2 and Supporting Information, Figure S6). Hapten **3** presented a face consisting of the bridgehead nitrogen, the aromatic ring, and the C-3 hydroxyl. Antibody recognition of the C-3 hydroxyl was stringent, not binding to the methyl ether at C-3 of codeine, oxycodone, and hydrocodone. Prescription opioid abuse and addiction are growing health problems and a strong risk factor leading to the use of heroin and drug addicts generally abuse multiple drugs.[50−52] Vaccine strategies combining multiple abused opioids like morphine, oxycodone, and hydrocodone have been proposed,[53,54] but these are inherently complex. The multispecificity of antibodies directed to TT−**1** indicates its potential as a single haptenic tool in an immunotherapeutic vaccine to combat abuse of heroin and other prescription opioid drugs.

It is essential that the antibodies induced by a heroin or opioid vaccine do not cross-react with the therapies for opioid abuse such as methadone, buprenorphine, and naltrexone.[51] The antibodies induced by both **1** and **3** did not react with these compounds, and more importantly the antibodies induced by either vaccine did not cross-react with naloxone, which is used as the overdose rescue treatment given intranasally to reverse respiratory depression due to heroin and other opioid overdose. This suggests that vaccination can be used together with standard therapies to prevent the withdrawal and craving symptoms associated with opioid withdrawal. Although the use of opioids for pain in addicts is highly debated, the poor binding of **1**-induced antibodies to methadone, tramadol, fentanyl, sufentanil, nalbuphine, and buprenorphine allows for their use in the event that an acute pain treatment is required for emergency use in vaccinated patients. The **1**-induced antibodies did not bind to any of the non-narcotic analgesics like acetylsalicylic acid, ibuprofen, and acetaminophen, which could also be used in immunized individuals for alternative pain management if needed.[52]

CONCLUSIONS

After a considerable amount of experimentation, a practical scalable synthesis of haptenic heroin surrogate **1** was completed in five steps from hydromorphone. The key improvement was the installation of the C-3 amido group using an activated phenol in a single transformation via water-promoted Buchwald−Hartwig cross coupling instead of a reduction/nitration/acylation sequence. This improvement enabled the synthesis of the most useful hapten, **1**, in 53% overall yield. Immunization with **1** conjugated to TT and mixed with ALF or ALFA as adjuvants protected mice and rats from subcutaneous and intravenous heroin challenge. The vaccine formulation induced partial efficacy from a 50 mg/kg heroin challenge dose, suggesting that it may be a valuable therapeutic to prevent heroin overdose. In addition, the cross-reactivity of the antibodies with other commonly abused prescription opioids suggests that the vaccine may have utility for these other opioids as well. The improved material throughput will enable the study and development of this hydrolytically stable conjugate heroin vaccine formulation using the hapten **1** for the treatment and prevention of heroin addiction. In conclusion, the TT−**1** heroin vaccine has great potential as a highly improved immunotherapeutic for addiction to heroin and other opioids that can be easily and effectively translated into humans as a synergistic approach to treat substance-use disorders.

EXPERIMENTAL SECTION

General Methods, Reagents, and Drugs. Microwave reactions were performed with a CEM Discover SP microwave synthesizer in either 10 or 35 mL reaction vessels. Melting points were determined on a Buchi B-545 instrument and are uncorrected. Proton and carbon nuclear magnetic resonance (^{1}H and ^{13}C NMR) spectra were recorded on a Varian Gemini-400 spectrometer in $CDCl_3$ (unless otherwise noted), with the values given in ppm (TMS as internal

DOI: 10.1021/acs.jmedchem.7b01427
J. Med. Chem. 2018, 61, 329−343

standard) and J (Hz) assignments of ^{1}H resonance coupling. Mass spectra (HRMS) were recorded on a VG 7070E spectrometer or a JEOL SX102a mass spectrometer using an electrospray ionization (ESI) source. The optical rotation data were obtained on a PerkinElmer polarimeter model 341 at room temperature. Gas chromatography (GC) was performed on an Agilent Technologies 6850 GC system equipped with a VL MSD detector. Thin layer chromatography (TLC) analyses were carried out on prepackaged plates using various gradients of $CHCl_3$/MeOH containing 1% of 28% NH_4OH (CMA) or gradients of EtOAc:*n*-hexane. Visualization was accomplished under UV light or by staining in an iodine chamber. Flash column chromatography was performed using RediSep Rf normal phase silica gel cartridges. Atlantic Microlabs, Inc., Norcross, GA, or Micro-Analysis, Inc., Wilmington, DE, performed elemental analyses, and the results were within ±0.4% of the theoretical values.

Tetanus toxoid (TT) was purchased from Statens Serum Institut (Copenhagen, Denmark). NHS-$(PEG)_2$-maleimide cross-linker [(SM-$(PEG)_2$] and dialysis cassettes (Slide-A-Lyzer G2, 10K MWCO) and Nunc MaxiSorp flat-bottom plates were purchased from Thermo Fisher Scientific (Rockford, IL). Dulbecco's phosphate buffered saline (PBS, 10 mM Na_2HPO_4, 1.8 mM KH_2PO_4, 2.7 mM KCl, 137 mM NaCl, pH 7.4) was purchased from Quality Biological Inc. (Gaithersburg, MD). Liposomal lipids consisting of 1,2-dimyristoyl-*sn*-glycero-3-phosphoglycerol (DMPG), 1,2-dimyristoyl-*sn*-glycero-3-phosphocholine (DMPC), monophosphoryl lipid A (PHAD or 3D-PHAD), and cholesterol (plant derived) were purchased from Avanti Polar Lipids (Alabaster, AL). Aluminum hydroxide adjuvant, Alhydrogel, was purchased from Brenntag (Denmark). Antimorphine BD1263 and anti-Tetanus Toxoid HYB-278-01 monoclonal antibodies were purchased from Abcam (Cambridge, MA). 3,6-Diacetylmorphine·HCl (heroin·HCl), 6-AM·HCl, M-3G·hydrate, M-6G·hydrate, normorphine·HCl·hydrate, hydrocodone, hydromorphone, oxymorphone, meperidine·HCl, fentanyl, sufentanil, and tramadol·HCl were purchased from Lipomed, Inc. (Cambridge, MA). Morphine sulfate salt·pentahydrate, codeine, oxycodone·HCl, levorphanol (+)-tartrate salt·dihydrate, nalbuphine·HCl·hydrate, methadone·HCl, buprenorphine·HCl, naloxone·HCl·dihydrate, naltrexone·HCl, acetylsalicylic acid, ibuprofen, and acetaminophen were purchased from Sigma-Aldrich (St. Louis, MO). Human opioid peptides β-endorphin and [Leu5]-enkephalin were purchased from AnaSpec (Fremont, CA).

Chemistry. *N-((4R,7S,7aR,12bS)-7-Acetamido-3-methyl-2,3,4,4a,5,6,7,7a-octahydro-1H-4,12- methanobenzofuro[3,2-e]-isoquinolin-9-yl)-3-(tritylthio)propanamide (**1**).* From **12**: Aniline **12** (0.170 g, 0.519 mmol) was dissolved in $CHCl_3$ (10 mL) and cooled to 0 °C. Triethylamine (0.420 g, 4.15 mmol, 0.580 mL, 8 equiv), 3-(tritylthio)propanoic acid (0.361 g, 1.03 mmol, 2 equiv), and TBTU (0.666 g, 2.07 mmol, 4 equiv) were added sequentially. The solution was stirred for 16 h, warming to 25 °C. The solution was washed with H_2O (2 × 5 mL) then brine (1 × 5 mL), dried over Na_2SO_4, filtered, and concentrated in vacuo to give a brown semisolid. The semisolid was purified by column chromatography on SiO_2 (98:1.8:0.2 to 90:9:1 $CHCl_3$:MeOH:28%NH_4OH) to give amide **1** (0.260 g, 76%) as a clear oil. The product was lyophilized with *t*-BuOH to give a white powder suitable for subsequent biological studies. HRMS (ESI^+) (m/z): [M + H] calcd for $C_{41}H_{44}N_3O_3S$ [M + H^+] 658.3103, found 658.3098. Anal. Calcd for $C_{41}H_{43}N_3O_3S$·*t*-BuOH: C, 73.84; H, 7.30; N, 5.74. Found C, 73.63; H, 7.39; N, 5.97.

*From Boc-Protected **19**.* To a solution of **19** (1.34 g, 3.14 mmol, free base) in $CHCl_3$ (10 mL) was added trifluoroacetic acid (5 mL) at room temperature, and the mixture was stirred for 3 h. The mixture was concentrated, and the residue was partitioned with $CHCl_3$ (20 mL) and saturated $NaHCO_3$ (20 mL). The layers were separated, and the aqueous layer was extracted with $CHCl_3$ (3 × 20 mL). The combined organic layers were dried over Na_2SO_4 and concentrated. To the resulting residue, $CHCl_3$ (20 mL) was added followed by triethylamine (875 μL, 6.28 mmol), COMU (1.6 g, 3.76 mmol), and 3-(tritylthio)propionic acid (1.3 g, 3.76 mmol) at ambient temperature under an atmosphere of argon. The solution was stirred for 30 min before quenching with H_2O (15 mL). The organic layer was separated, and the aqueous layer was extracted with $CHCl_3$ (4 × 20 mL). The combined organic layers were dried over Na_2SO_4 and concentrated. The residue was purified by column chromatography using a gradient of 0−15% MeOH/5% NH_4OH in $CHCl_3$, yielding pure (by NMR) product **1** as a light-yellow oil (1.7 g, 82% from **19**). To remove the color impurity, the oil was further purified by column chromatography using a RediSep Rf Gold Cyano functionalized column and a mixture of H_2O and acetonitrile as a mobile phase. Fractions containing the product were combined and the solvents removed, affording **1** as a colorless oil (1.3 g). The oil was further formulated into a white powder after dissolving it in a mixture of MeOH, *tert*-butanol, and H_2O (1:12:3), followed by a freeze-dry process. ^{1}H NMR ($CDCl_3$) δ 7.41−7.43 (m, 6H), 7.27 (t, 6H, J = 7.34 Hz), 7.19 (t, 4H, J = 7.34 Hz), 6.94 (s, 1H), 6.62 (d, 1H, J = 8.32 Hz), 6.42 (d, 1H, J = 9.29 Hz), 4.60 (d, 1H, J = 4.89 Hz), 4.15- 4.23 (m, 1H), 3.08 (dd, 1H, J = 6.11 and 2.69 Hz), 2.95 (d, 1H, J = 19.07 Hz), 2.54−2.60 (m, 2H), 2.37−2.49 (m, 2H), 2.36 (s, 3H), 2.15−2.30 (m, 4H), 1.90 (dd, 1H, J = 12.72 and 5.38 Hz), 1.83 (s, 3H), 1.62−1.74 (m, 2H), 1.38−1.41 (m, 1H), 0.79−1.01 (m, 2H). ^{13}C NMR ($CDCl_3$): δ 169.5, 169.1, 150.5, 144.6, 133.2, 130.1, 129.5, 127.9, 126.7, 123.2, 119.2, 117.1, 90.8, 66.9, 59.8, 46.3, 46.1, 43.1, 42.6, 36.9, 36.0, 35.9, 27.5, 23.4, 22.8, 20.5, 20.1. HRMS-ESI (m/z): $[M + H]^+$ calcd for $C_{41}H_{44}N_3O_3S$ 658.3103, found 658.3107. Anal. Calcd for $C_{41}H_{43}N_3O_3S$ 0.45 *tert*-butanol·1.0H_2O: C, 72.48; H, 7.03; N, 5.92. Found: C, 72.51; H, 6.88; N, 5.74.

*N-((7aR)-9-Amino-3-methyl-2,3,4,4a,5,6,7,7a-octahydro-1H-4,12-methanobenzofuro[3,2-e] isoquinolin-7-yl) Acetamide (**12**).* Amide **13** (0.60 g, 1.63 mmol) was dissolved in 1 N HCl (32 mL) and heated to 60 °C for 72 h. The reaction mixture was made basic (pH > 9) with 28% NH_4OH. The solution was extracted with 10% *i*-PrOH/$CHCl_3$ (3 × 50 mL), and the organic layer was dried over Na_2SO_4, filtered, and concentrated in vacuo to give a yellow oil. The oil was purified by column chromatography on SiO_2 (95:4.5:0.5 to 85:13.5:1.5 $CHCl_3$:MeOH:28% NH_4OH) to give aniline **12** (0.46 g, 86%) as a clear oil that was identical to previous reports.[14] $[\alpha]_D^{20}$ = −120.7 (c = 0.46, MeOH). ^{1}H NMR (400 MHz, $CDCl_3$) δ 6.46 (d, J = 8.0 Hz, 1H), 6.44 (d, J = 8.0 Hz, 1H), 5.93 (d, J = 8.8 Hz, 1H), 4.51 (d, J = 4.4 Hz, 1H), 4.15 (qd, J = 11.6, 4.4 Hz, 1H), 3.53 (s, 2H), 2.99 (dd, J = 6.0, 2.4 Hz, 1H), 2.86 (d, J = 18.4 Hz, 1H), 2.39 (dd, J = 12, 4 Hz, 1H), 2.30 (s, 3H), 2.26−2.15 (m, 3H), 1.87 (s, 3H), 1.81 (td, J = 12.0, 4.8 Hz, 1H), 1.62−1.54 (m, 2H), 1.36 (m, 1H), 0.96 (m, 1H), 0.81 (m, 1H). ^{13}C NMR (100 MHz, $CHCl_3$) δ 169.4, 146.0, 128.6, 127.1, 125.5, 119.26, 116.6, 89.5, 59.6, 46.6, 46.3, 43.1, 42.7, 37.4, 36.9, 23.3, 22.5, 20.3, 19.8.

*N,N′-((7S,7aR)-3-Methyl-2,3,4,4a,5,6,7,7a-octahydro-1H-4,12-methanobenzofuro[3,2-e]isoquinoline-7,9-diyl) Diacetamide (**13**).* Amine **16** (1.77 g, 4.24 mmol, contaminated with ∼10% benzylamine) was dissolved in EtOH (40 mL) in a 250 mL pressure tested reaction bottle. Escat 103 5% Pd/C (0.590 g, 33% w/w of **16**) was added, and the vessel was pressurized to 50 psi H_2 in a Parr shaker. The reaction mixture was heated to 50 °C and then shaken for 24 h, after which an additional 0.590 g of Escat 103 was added. The vessel was repressurized to 50 psi H_2 and shaken at 50 °C until starting material was consumed as indicated by GC/MS analysis. The reaction mixture was cooled to 25 °C, filtered through Celite, and concentrated in vacuo to give a yellow oil (**17**). The resulting oil was dissolved in $CHCl_3$ (40 mL) and cooled to 0 °C. Triethylamine (2.57 g, 3.55 mL, 25.43 mmol, 6 equiv) and acetic anhydride (0.87 g, 0.80 mL, 8.48 mmol, 2 equiv) were added sequentially, and the solution was stirred 16 h, warming to 25 °C. The solution was washed with 28% NH_4OH, dried over Na_2SO_4, and concentrated in vacuo to give a yellow oil. The oil was purified via column chromatography on SiO_2 (95:4.5:0.5 90:9:1 $CHCl_3$:MeOH:28% NH_4OH) to give a yellow solid. The solid was triturated in EtOAc to give amide **13** as a white solid (1.29 g, 67% over three steps from **15**), which was identical to previous reports.[17] IR (ATR) 1672, 1646 cm^{-1}; mp 265 °C (dec). ^{1}H NMR (400 MHz, $CDCl_3$) δ 7.21 (s, 1H), 6.66 (d, J = 8.0 Hz, 1H), 6.42 (d, J = 8.8 Hz, 1H), 4.63 (d, J = 4.8 Hz, 1H), 4.23 (ddd, J = 16.8, 9.6, 4.4 Hz, 1H), 3.10 (dd, J = 6.0, 2.8 Hz, 1H), 2.98 (d, J = 18.8 Hz, 1H), 2.79 (dd, J = 12.4, 4.0 Hz, 1H), 2.41 (dd, J =

DOI: 10.1021/acs.jmedchem.7b01427
J. Med. Chem. 2018, 61, 329−343

19.2, 6.4 Hz, 1H), 2.38 (s, 3H), 2.29 (td, J = 9.2, 2.8 Hz, 1H), 2.22 (td, J = 12.4, 3.2 Hz, 1H), 2.17 (s, 3H), 1.97 (s, 3H), 1.92 (td, J = 8.4, 5.2 Hz, 1H), 1.75−1.65 (m, 2H), 1.42 (td, J = 9.2, 4.0 Hz, 1H); 1.024 (m, 1H), 0.87 (m, 1H). ^{13}C NMR (100 MHz, $CDCl_3$) δ 169.5, 168.2, 150.4, 133.0, 129.9, 123.2, 119.2, 117.6, 90.7, 59.8, 46.4, 46.1, 43.1, 42.6, 36.9, 36.3, 23.9, 23.6, 22.9, 20.4, 20.1.

*N,N′-((7S,7aR)-2,3,4,4a,5,6,7,7a-Octahydro-1H-4,12-methanobenzofuro[3,2-e]isoquinoline-7,9-diyl)diacetamide (**14**).*[24] To a solution of **13** (7 mg, 0.019 mmol) in 1,2-dichloroethane 0.25 mL was added K_2CO_3 (0.250 mg) and ethyl chloroformate (0.013 g, 0.12 mmol, 0.012 mL, 5 equiv). The mixture was heated to reflux for 1.5 h until the starting material was consumed as indicated by TLC (90:9:1 $CHCl_3$:MeOH:28% NH_4OH) to give the ethyl carbamate as indicated by GC/MS. The solution was cooled to 25 °C, filtered, and concentrated in vacuo to give a yellow oil. The oil was dissolved in 1,2-dichloroethane (0.25 mL), and trimethylsilyl iodide (0.012 g, 0.060 mmol, 0.009 mL, 2.5 equiv) in 1,2-dichloroethane (0.10 mL) was added. The solution was heated to 55 °C for 1 h and cooled to 25 °C, and additional trimethylsilyl iodide (0.024 g, 0.12 mmol, 0.018 mL, 5 equiv) was added. The solution was heated to 55 °C for 14 h, then heated to reflux for 4 h until the ethyl carbamate was consumed as indicated by TLC. The solution was cooled to 25 °C, diluted with $CHCl_3$ (10 mL), and stirred with saturated aq $Na_2S_2O_3$ (10 mL) until homogeneous layers were visible. The solution was made basic (pH > 9) with 28% NH_4OH. The organic layer was separated, and the aqueous layer was extracted with $CHCl_3$ (3 × 10 mL). The combined organic layers were dried over Na_2SO_4, concentrated in vacuo, and purified via column chromatography on SiO_2 (98:1.8:0.2 to 90:9:1 $CHCl_3$:MeOH:28% NH_4OH) to give **14** as a clear oil (4.4 mg, 65%) that was identical to previous reports.

*N-((7aR)-3-Methyl-7-oxo-2,3,4,4a,5,6,7,7a-octahydro-1H-4,12-methanobenzofuro[3,2-e]isoquinolin-9-yl) Acetamide (**15**). Microwave Heating Method.* A 35 mL microwave reactor vessel equipped with a magnetic stir bar was charged with triflate **5** (1.39 g, 3.33 mmol), freshly ground K_3PO_4 (0.78 g, 3.66 mmol, 1.1 equiv), acetamide (0.47 g, 7.33 mmol, 2.2 equiv), *tert*-butanol (15 mL), and H_2O (0.060 g, 0.060 mL, 3.33 mmol, 1 equiv). The vessel was capped with a Teflon seal and flushed with argon. *tert*-Butyl BrettPhos palladacycle precatalyst (Table 1) (0.14 g, 0.17 mmol, 0.05 equiv) was added in one portion, and the solution was heated in the microwave to 110 °C for 2 h to give a dark-brown suspension. The suspension was diluted with hexanes concentrated in vacuo to give a black solid. The solids were taken up in 10% MeOH/$CHCl_3$ (100 mL), washed with H_2O (2 × 50 mL), dried over Na_2SO_4, and concentrated to give a black oil. The oil was purified via column chromatography on SiO_2 (95:4.5:0.5 to 88:10.8:1.2 $CHCl_3$:MeOH:28% NH_4OH) to give a brown solid. The solid was triturated with EtOAc to give acetamide **15** (0.80 g, 73%) as an off-white solid.

Conventional Heating Method. A mixture of triflate **5** (8 g, 19.16 mmol), acetamide (2.49 g, 42.15 mmol), and potassium phosphate (4.47 g, 21.07 mmol) was purged with argon for 15 min. *tert*-Butyl BrettPhos palladacycle catalyst (Table 1) (0.818 g, 0.958 mmol) was then added, and the solids were purged with argon for additional 15 min. Degassed *tert*-butanol (110 mL) and degassed H_2O (0.4 mL) were added to the solids, and the reaction mixture was heated to 90 °C for 4 h under an atmosphere of argon. The solvent was removed in vacuo, and the resulting residue was partitioned with a mixture of 10% isopropyl alcohol in $CHCl_3$ (80 mL) and H_2O (60 mL) and separated. The aqueous layer was further extracted with a mixture of 10% isopropyl alcohol in $CHCl_3$ (3 × 80 mL). The combined organic layers were dried over Na_2SO_4 and concentrated. The residue was purified by column chromatography using a gradient of 0−12% MeOH/5% NH_4OH in $CHCl_3$, yielding the title compound **15** as a light-brown solid (5.5 g, 88%). ^{1}H NMR ($CDCl_3$) δ 7.90 (d, 1H, J = 8.31 Hz), 7.34 (bs, 1H), 6.67 (d, 1H, J = 8.31 Hz), 4.63 (s 1H), 3.16 (dd, 1H, J = 5.38 and 2.93 Hz), 3.03 (d, 1H, J = 19.08 Hz), 2.51−2.58 (m, 2H), 2.26−2.42 (m, 6H), 2.13−2.19 (m, 4H), 2.04 (dt, 1H, J = 12.22 and 4.4 Hz), 1.71−1.85 (m, 2H), 1.16−1.26 (m, 1H). ^{13}C NMR ($CDCl_3$): δ 208.1, 168.2, 146.4, 129.6, 125.6, 121.1, 120.5, 119.7, 91.5, 59.1, 46.8, 46.6, 42.8, 42.7, 40.2, 35.5, 25.2, 24.4, 20.2. HRMS-ESI (m/z): $[M + H]^+$ calcd for $C_{19}H_{23}N_2O_3$ 327.1703, found 327.1703.

*N-((7S,7aR,12bS)-7-(Benzylamino)-3-methyl-2,3,4,4a,5,6,7,7a-octahydro-1H-4,12- methanobenzofuro[3,2-e]isoquinolin-9-yl) Acetamide (**16**).* Ketone **15** (2.17 g, 6.65 mmol), THF (66 mL), *N*,*N*-diisopropylethylamine (2.58 g, 3.48 mL, 19.95 mmol, 3 equiv), benzylamine (0.75 g, 0.76 mL, 6.98 mmol, 1.05 equiv), and $MgSO_4$ (1.60 g, 13.30 mmol, 2 equiv) were added, and the suspension was stirred at 25 °C for 1 h. Sodium triacetoxyborohydride (2.82 g, 13.3 mmol, 2 equiv) was then added in one portion. The mixture was stirred for 16 h at 25 °C. Unreacted starting material and unreduced imine were detected by GC/MS, thus additional benzylamine (0.11 g, 0.10 mmol, 0.11 mL, 0.15 equiv), $MgSO_4$ (0.800 mg, 6.65 mmol, 1 equiv), and sodium triacetoxyborohydride (1.41 g, 6.65 mmol, 1 equiv) were added and the reaction was stirred for 24 h. The suspension was filtered, and the filtrate was concentrated in vacuo to give a yellow semisolid. The semisolid was dissolved in $CHCl_3$ (200 mL), washed with saturated aq $NaHCO_3$ (2 × 50 mL), dried over Na_2SO_4, filtered, and concentrated in vacuo to give a yellow oil. The oil was purified via column chromatography (99:0.9:0.1 $CHCl_3$:MeOH:28% NH_4OH to 95:4.5:0.5 $CHCl_3$:MeOH:28% NH_4OH) to give **16** (2.03 g, 72%) as a yellow oil contaminated with ∼10% benzylamine, which was used without further purification. Two analytical samples were prepared, the first by repeated column chromatography on SiO_2 as described to remove the trace benzylamine, the second by dissolving impure **16** in MeOH, adding oxalic acid (2 equiv) and concentrating the solution to give a white solid. The solid was recrystallized from EtOAc:MeOH then *i*-PrOH:MeOH to give **16** oxalate salt. IR (ATR, free base) 1667 cm^{-1}; $[\alpha]^{20}$ = −139.0° (c = 5.15, CHCl free base). ^{1}H NMR (400 MHz, $CDCl_3$, free base) δ 7.38−7.29 (m, 5H), 7.26−7.22 (m, 1H), 6.62 (d, J = 8.0 Hz, 1H), 4.76 (d, J = 3.6 Hz, 1H), 3.86 (s, 2H), 3.06 (dd, J = 6.4, 2.8 Hz, 1H), 2.96 (d, J = 18.8 Hz, 1H), 2.79 (td, J = 12.4, 3.6 Hz, 1H), 2.46 (dd, J = 12.0 4.4 Hz, 1H), 2.37 (dd, J = 18.8, 2.4, 1H), 2.36 (s, 3H), 2.25 (td, J = 12.4, 3.6 Hz, 1H), 2.18 (td, J = 10.0, 2.8 Hz, 1H), 2.11 (s, 3H), 1.88 (td, J = 12.4, 5.2 Hz, 1H), 1.69−1.53 (m, 3H), 0.89−0.82 (m, 2H). ^{13}C NMR (100 MHz, $CDCl_3$, free base) δ 168.2, 148.8, 140.3, 131.5, 129.1, 128.5. 128.2, 127.1, 121.4, 118.9, 118.7, 91.5, 59.7, 54.3, 50.8, 46.2, 43.3, 42.8, 38.0, 36.6, 24.4, 21.5, 20.8, 20.3. HRMS (ESI$^+$) (m/z): $[M^+ + H]$ calcd for $C_{26}H_{32}O_2N_3$ 418.2489, found 418.2488. Anal. Calcd for $C_{26}H_{31}O_2N_3$·1.5 oxalic acid·2H_2O·0.5 CH_3OH) C, 58.60; H, 6.67; N, 6.95. Found C, 58.44, H, 6.67; N, 6.81.

*tert-Butyl ((7aR,12bS)-3-Methyl-7-oxo-2,3,4,4a,5,6,7,7a-octahydro-1H-4,12-methanobenzofuro[3,2-e]isoquinolin-9-yl)carbamate (**18**).* Compound **15** (4.2 g, 12.86 mmol) was dissolved in 1 N HCl (85 mL) and heated to 60 °C for 48 h. The reaction mixture was cooled to room temperature, and the pH was carefully brought to 6.5−7.0, first with 20% NaOH and then 5% NaOH. Di-*tert*-butyl dicarbonate (7.38 mL, 32.15 mmol) was added, and the mixture was stirred overnight at room temperature. The aqueous layer was extracted with $CHCl_3$ (4 × 80 mL). The combined organic layers were washed with 1% NaOH (100 mL), dried over Na_2SO_4, and concentrated, yielding a light-yellow foam (4.8 g, 98%). The crude product **18** was directly used in the next step of synthesis. ^{1}H NMR ($CDCl_3$) δ 7.72 (bs, 1H), 6.65−6.67 (m, 2H), 4.61 (s, 1H), 3.16 (dd, 1H, J = 5.64 and 2.35 Hz), 3.01 (d, 1H, J = 18.78 Hz), 2.51−2.57 (m, 2H), 2.25−2.44 (m, 6H), 2.17 (dt, 1H, J = 11.74 and 2.93 Hz), 2.04 (dt, 1H, J = 11.74 and 4.69 Hz), 1.73−1.84 (m, 2H), 1.48 (s, 9H), 1.17−1.28 (m, 1H). ^{13}C NMR ($CDCl_3$): δ 208.1, 152.7, 145.9, 128.1, 125.5, 121.0, 119.7, 119.4, 91.4, 80.3, 59.2, 46.7, 46.6, 42.9, 42.8, 40.3, 35.5, 28.3, 25.2, 20.0. HRMS-ESI (m/z): $[M + H]^+$ calcd for $C_{22}H_{29}N_2O_4$ 385.2127, found 385.2128.

*tert-Butyl ((7S,7aR,12bS)-7-Acetamido-3-methyl-2,3,4,4a,5,6,7,7a-octahydro-1H-4,12-methanobenzofuro[3,2-e]-isoquinolin-9-yl)carbamate (**19**).* To a mixture of **18** (4 g, 10.4 mmol) and ammonia solution in ethanol (2M, 52 mL, 104 mmol) was added titanium(IV) isopropoxide (6.16 mL, 20.8 mmol) at ambient temperature under an atmosphere of argon. The flask was capped, and stirring was continued overnight. Sodium borohydride (0.59 g, 15.6

DOI: 10.1021/acs.jmedchem.7b01427
J. Med. Chem. 2018, 61, 329−343

mmol) was then added at 8 °C, and the mixture was allowed to warm to room temperature while being stirred for an additional 3 h. The reaction was quenched by adding NH_4OH (2M, 45 mL) followed by Celite (10 g) in order to facilitate filtration of solids. The solids were filtered off and washed with dichloromethane. The organic layer was separated, and the remaining aqueous layer was extracted with dichloromethane (3 × 20 mL). The combined organic extracts were dried over Na_2SO_4 and concentrated in vacuo to give a light-yellow foam. The resulting residue was dissolved in anhyd EtOAc (10 mL), and acetic anhydride (1.47 mL, 15.6 mmol) was added. Almost immediately, a white solid precipitated out. The mixture was stirred for 1 h, and the white solid was filtered off, washed with diethyl ether, and dried in vacuo, yielding **19** (2.57 g). The remaining mother liquor was basified with saturated $NaHCO_3$, and the aqueous layer was extracted with $CHCl_3$ (3 × 40 mL). The combined organic layers were concentrated, and the residue was purified by column chromatography using a gradient of 0−10% MeOH/5% NH_4OH in $CHCl_3$, yielding an additional amount of **19** (78% free base, over 3 steps from **18**). ^{1}H NMR ($CDCl_3$) δ 7.29 (d, 1H, J = 8.2 Hz), 6.64 (d, 1H, J = 8.2 Hz), 6.35 (m, 1H), 6.23 (bs, 1H), 4.61 (d, 1H, J = 4.1 Hz), 4.20−4.26 (m, 1H), 3.08 (m, 1H), 2.94 (d, 1H, J = 18.8 Hz), 2.37−2.48 (m, 2H), 2.36 (s, 3H), 2.17−2.29 (m, 2H), 1.96 (s, 3H), 1.87−1.93 (m, 1H), 1.63−1.74 (m, 2H), 1.50 (s, 9H), 1.42 (m, 1H), 0.83−0.99 (m, 2H). ^{13}C NMR ($CDCl_3$): δ 169.4, 152.9, 149.3, 131.6, 129.5, 121.8, 119.2, 118.0, 90.5, 80.4, 59.7, 46.4, 46.1, 43.1, 42.6, 37.1, 36.4, 28.4, 23.4, 22.8, 20.4, 19.9. HRMS-ESI (m/z): $[M + H]^+$ calcd for $C_{24}H_{34}N_3O_4$ 428.2549, found 428.2548. Anal. Calcd for $C_{24}H_{33}N_3O_4$: C, 67.42; H, 7.78; N, 9.83. Found: C, 67.04; H, 7.73; N, 9.77.

*tert-Butyl ((4bS,6S)-6-Acetamido-4-hydroxy-11-methyl-6,7,8,8a,9,10-hexahydro-5H-9,4b-(epiminoethano)phenanthren-3-yl)carbamate (**20**).* A mixture of **18** (576.7 mg, 1.5 mmol), ammonium formate (1.26 g, 20 mmol), and 10% Pd-C (60 mg) was purged with argon for 10 min. Degassed MeOH (5 mL) and degassed H_2O (0.6 mL) were added to the solids, and the reaction mixture was heated to 65 °C for 2 h under an atmosphere of nitrogen. The catalyst was filtered through a pad of Celite and washed with MeOH. The solvents were removed in vacuo, and the resulting yellow oil was taken in with NH_4OH solution (2 M, 10 mL) and extracted with $CHCl_3$ (4 × 15 mL). The combined organic layers were dried over Na_2SO_4 and concentrated in vacuo. The residue was dissolved in anhydrous EtOAc (5 mL) and acetic anhydride (212 μL, 2.25 mmol) was added and the mixture was stirred for 1 h at room temperature. The reaction was quenched by pouring into an NH_4OH solution (2M, 8 mL), and the aqueous layer was extracted with EtOAc (4 × 8 mL). The combined organic layers were concentrated, and the residue was purified by column chromatography using a gradient of 0−12% MeOH/5% NH_4OH in $CHCl_3$, followed by additional column chromatography using a neutral alumina column to give **20** (231 mg, 52%). The free base was converted to its hydrochloride salt by treating ethanolic solution of **20** with 1 equiv of an anhydrous solution of HCl in Et_2O. ^{1}H NMR ($CDCl_3$): free base, δ 6.81−6.83 (m, 2H), 6.69 (d, 1H, J = 8.32 Hz), 5.53 (d, 1H, J = 7.83 Hz), 4.22−4.25 (m, 1H), 3.74−3.78 (m, 1H), 2.92 (d, 1H, J = 18.59 Hz), 2.80−2.82 (m, 1H), 2.72 (dd, 1H, J = 18.59 and 5.87 Hz), 2.41−2.44 (m, 1H), 2.34 (s, 3H), 1.95−2.02 (m, 1H), 1.88−1.91 (m,1H), 1.72−1.79 (m, 2H), 1.52−1.64 (m, 6H), 1.48 (s, 9H), 1.32−1.40 (m, 2H). ^{13}C NMR ($CDCl_3$): δ 169.4, 155.5, 148.1, 137.3, 130.1, 124.4, 121.1, 120.6, 82.2, 57.4, 47.2, 46.7, 45.7, 42.6, 38.6, 37.9, 36.5, 30.8, 28.2, 24.7, 23.3, 22.6. LRMS-ESI (m/z): $[M + H]^+$ 430.0.

Biology. *Heroin Conjugate Vaccine Synthesis.* The heroin haptens **1** and **3** were coupled to the tetanus toxoid (TT) carrier protein using optimized coupling procedures.[14,55] Briefly, TT was incubated with the $SM(PEG)_2$ crosslinker at a molar ratio of 1:1600 for 2 h, processed, and quantified.[14,55] Deprotected haptens were mixed with TT with a TT:hapten molar ratio of 1:300. Excess haptens were removed by overnight dialysis against PBS, pH 7.4, at 4 °C. The TT−hapten conjugates were sterile filtered and quantified by BCA. The number of haptens attached per TT molecule was quantified by MALDI-TOF mass spectrometry (Supporting Information, Figure S1), and protein integrity was verified via gel electrophoresis (Supporting Information, Figure S2).

Vaccine Formulations and Rodent Immunization. Army Liposome Formulations (ALF) consisting of DMPC:cholesterol:DMPG in molar ratio of 9:7.5:1 and monophosphoryl lipid A (PHAD or 3D-PHAD) as adjuvant were prepared by lipid deposition.[38,45,46] Lipids were mixed and dried by rotary evaporation. Multilamellar liposomal vesicles (MLV) were formed by adding PBS, pH 7.4, to get the desired final concentration of total phospholipids. The MLV were microfluidized using a Microfluidics LV1 low volume high shear microfluidizer (Microfluidics, Westwood, MA) at 30000 psi to form small unilamellar liposomal vesicles (SUV).[38]

All animal studies were conducted under an approved animal use protocol in an AAALACi accredited facility in compliance with the Animal Welfare Act and other federal statutes and regulations relating to animals and experiments involving animals and adheres to principles stated in the *Guide for the Care and Use of Laboratory Animals*, NRC Publication, 2011 edition. For mouse studies (Supporting Information, Figure S3), ALF was mixed with TT−**1** or TT−**3** to give a final vaccine formulation consisting of SUV with a 1:8.8 molar ratio of MPLA to phospholipids with 10 μg of protein antigens and 20 μg of MPLA (PHAD) per mouse vaccine dose of 50 μL in PBS, pH 7.4. Female Balb/c mice (7 weeks of age; 10 per group) from Jackson Laboratories (Bar Harbor, ME) were immunized intramuscularly (IM) at weeks 0, 3, 6, and 14 in alternating rear thighs. The mice were challenged after three vaccinations at weeks 10 with subcutaneous (SC) heroin (1 mg/kg) and then later repeatedly after four vaccinations at weeks 16 and 17 with intravenous (IV) heroin (0.5 mg/kg). All mice were bled prior to each vaccination and prior to the first challenge at week 8. At week 20, the mice were euthanized and the blood was collected by cardiac puncture.

For rat studies (Supporting Information, Figure S5), ALF was mixed with TT−**1** to give a final vaccine formulation consisting of SUV with a 1:8.8 molar ratio of MPLA to phospholipids with 100 μg TT−**1** antigen and 200 μg of MPLA (3D-PHAD) per rat vaccine dose of 200 μL in PBS, pH 7.4. Male Sprague−Dawley rats (9 weeks of age; ∼250 g weight; 8 per group) from Charles River Laboratories (Wilmington, MA) were immunized using a similar schedule as mice except that the last challenge at week 17 was SC. At week 27, the rats were euthanized and the blood was collected by cardiac puncture.

For the high heroin dose challenge study (Figure 6), mice (n = 10) were immunized at weeks 0, 3, and 6 with 10 μg of TT−**1** formulated with ALF + aluminum hydroxide [ALFA] as adjuvant[42,43] that contained SUV with 1:8.8 molar ratio of 3D-PHAD to phospholipids and 30 μg of aluminum (Alhydrogel). For the ALFA adjuvant formulations, the TT−**1** antigen was first adsorbed on Alhydrogel for 1 h and then mixed with ALF. The SUV for this study were lyophilized, whereas for all previous studies they were not lyophilized. The mice were bled at week 8 and challenged along with unvaccinated controls at week 10 with 50 mg/kg SC heroin and the locomotion was monitored for 30 min before and after challenge as described below.

Antibody Titer and Affinity Measurements. For binding ELISA, Nunc MaxiSorp flat-bottom plates were coated with the BSA−**1**, BSA−**3**, or TT (0.1 μg/0.1 mL/well in PBS) and the ELISA was processed.[14] Serum IgG concentrations were quantified for both mouse and rat samples using corresponding standard curves of murine antimorphine monoclonal antibody (mAb), anti-TT mAb for TT (Figure S4), and haptens (Figure S18) as described in Supporting Information.

For competition ELISA, mouse and rat sera from week 8 were diluted in 1% BSA in TBS (20 mM Tris, 154 mM sodium chloride, pH 7.4) blocker to give an ELISA absorbance of ∼1.5. The various competitive drugs were diluted in log order concentrations in a 96-well plate and mixed with diluted sera to give final inhibitor concentrations between 0.01 and 1000 μM. The point at 0 μM corresponded to the negative control. After 30 min incubation at room temperature, the serum−inhibitor mixture was added to the BSA−hapten coated and blocked ELISA plates, which were processed similarly to the binding ELISA in the Supporting Information.[14,18,24] The 50% inhibitory concentration (IC_{50} value) of each compound

DOI: 10.1021/acs.jmedchem.7b01427
J. Med. Chem. 2018, 61, 329−343

was calculated from its normalized ELISA curve for individual animals and pooled sera from each group (Supporting Information, Table S1 and Table S2).

Heroin Challenge and Vaccine Efficacy Assessments. Both Balb/c mice and Sprague–Dawley rats were repeatedly challenged with heroin·HCl in saline either by SC route with 1 mg/kg injected between the front shoulders or by IV route with 0.5 mg/kg injected in the tail vein. For each assay, the responses before heroin injection (pre, baselines) and 20 min after heroin injection (post) were measured.

Vaccine efficacy in mice was measured by tail flick antinociception assay (Figure 5, top panel)[14,56,57] and locomotion analysis (Figure 5, bottom panel).[49] For the tail flick test, an infrared light was focused on the tail 3 cm from the tip using the tail flick analgesia meter (Harvard Apparatus, Holliston, MA). The time from the onset of the heat to the withdrawal of the tail (latency) was measured. Baseline latencies were between 2 and 4 s. To avoid burns, the heat stimulus was discontinued after 8 s (cutoff latency). The latency data (antinociception) were converted to percent of maximum possible effect (%MPE) as follows:

$$\%\mathrm{MPE} = 100 \times (\text{post heroin injection latency time} - \text{baseline latency time})/(\text{cutoff latency} - \text{baseline latency time})$$

Movement of mice was recorded by overhead video camera for 5 min after the tail flick assay and analyzed using EthoVision XT software (Noldus Information Technology Inc., Leesburg, VA) to measure the total distance moved (cm) and mean velocity (cm/s) for each animal. Mice were acclimated in the locomotion chambers for 30 min prior to the day of heroin challenge.

For rats, the warm water tail immersion assay was used instead of the tail flick assay (Figure 8, top panel).[57] The rat tail was immersed 6 cm from the tip in the immersion test analgesia meter (IITC Life Science, Woodland Hills, CA) set at 54 °C. The latency times were measured with cutoff as 10 s and antinociception, measured as % MPE, were calculated as above. Unlike mice, heroin administration sedated the unvaccinated control rats and reduced their overall movement. Hence, instead of the locomotion assay, the BIO-T2CT thermal place preference, two-temperature zone choice Test (TPPT) with DHCP detection software (Bioseb, EB Instruments, Pinellas Park, FL) was used (Figure 8, bottom panel).[58] The TPPT consisted of two hot/cold plates (165 × 165 mm^2 each) placed side by side so that the adjacent thermal surfaces formed a single open-topped enclosure. One plate was set at ambient temperature of 25 °C, whereas the other plate was set at hot temperature of 54 °C. The rat was gently placed on the hot side and allowed to move freely from plate to plate for 3 min. Movements were recorded by an overhead infrared camera. Rats that spent more than 30 s uninterrupted on the hot side at a stretch were removed to avoid burns and were scored as 100% on the hot side. The number of crossings between the two plates, and the percentage of time spent on the hot plate were calculated for each animal. Before beginning the experiments, the rats were trained for 5 min a day for 2 days by setting both the plates at 25 °C and ensuring that the rats spent approximately the same amount of time on each plate.

Data Analysis. Computational and statistical analysis were performed using GraphPad Prism. All values are reported as mean ± SEM. Antibody titers were expressed as μg/mL serum, as interpolated from the corresponding standard curves of murine monoclonal antibodies using sigmoidal, four-parameter nonlinear regression curve fit. For calculation of the IC_{50} values for various drugs, the competition ELISA data were first normalized to correct for the different absorbances of the no inhibitor samples by calculating the percent binding. The normalized competition curves were then fitted with the log(inhibitor) vs normalized response–variable slope regression to calculate the IC_{50} values. Statistical comparison between the controls and the TT–**1** and TT–**3** vaccinated groups was performed using one-way ANOVA, Kruskal–Wallis test with Dunn's correction for multiple comparisons (Figure 5). The overtime data between two groups was compared using two-way ANOVA with Sidak's multiple comparisons test (Figure 6). The data between two groups was compared using Mann–Whitney nonparametric *t* test (Figure 8). The asterisk(s) and corresponding *p* values were: (1) *, $p < 0.05$; **, $p < 0.01$; ***, $p < 0.001$; using one-way ANOVA and Kruskal–Wallis test with Dunn's correction for multiple comparison. (2) *, $p < 0.05$; ***, $p < 0.001$; ****, $p < 0.0001$; using two-way ANOVA with Sidak's multiple comparisons test. (3) *, $p < 0.05$; **, $p < 0.01$; ***, $p < 0.001$; using Mann–Whitney nonparametric *t* test.

■ ASSOCIATED CONTENT

Supporting Information

The Supporting Information is available free of charge on the ACS Publications website at DOI: 10.1021/acs.jmedchem.7b01427.

MALDI-TOF MS, SDS-PAGE, and native gels, and ELISA data for the TT-**1** and TT-**3** conjugates; ^{1}H and $^{13}CNMR$ spectra of novel compounds; microanalytical data and crystallographic data for **19** and **20** (PDF)

Molecular formula strings (CSV)

■ AUTHOR INFORMATION

Corresponding Authors

*For G.R.M.: phone, 301-319-9973; fax, 301-319-7518; E-mail, gmatyas@hivresearch.org.

*For K.C.R.: phone, 301-217-5200; fax, 301-217-5214; Email, kennerr@mail.nih.gov.

ORCID

Gary R. Matyas: 0000-0002-2074-2373

Notes

Material has been reviewed by the Walter Reed Army Institute of Research. There is no objection to its presentation and/or publication. The opinions or assertions contained herein are the private views of the authors, and are not to be construed as official, or as reflecting true views of the Department of the Army, the Department of Defense, NIDA, NIH or the US government.

The authors declare the following competing financial interest(s): GRM, KCR, AEJ, and CRA are co-inventors in a related US patent owned by the US Army and NIDA, and that is licensed to Opiant Pharmaceuticals.

■ ACKNOWLEDGMENTS

The work of A.S., J.F.G.A., A.E.J., and K.C.R. was supported by the NIH Intramural Research Programs of the National Institute on Drug Abuse and the National Institute of Alcohol Abuse and Alcoholism, The work of G.R.M., O.B.T., R.J., Z.B., and C.R.A. was supported through a Cooperative Agreement Award (no. W81XWH-07-2-067) between the Henry M. Jackson Foundation for the Advancement of Military Medicine and the U.S. Army Medical Research and Materiel Command (MRMC). The work was partially supported by an Avant Garde award to GRM from NIDA (NIH grant no. 1DP1DA034787-01). The X-ray crystallographic work was supported by NIDA through an Interagency Agreement no. Y1-DA1101 with the Naval Research Laboratory (NRL), NIH, DHHS. We thank Dr. John Lloyd and Noel Whittaker (Mass Spectrometry Facility, NIDDK) for the mass spectral data. We thank Alexander Duval, Courtney Tucker, Sarah Claire Kim, Marcus Gallon, Caroline Kittinger, SPC Ye Seul Kotorobay, and Enrique Alonso for providing technical assistance.

DOI: 10.1021/acs.jmedchem.7b01427
J. Med. Chem. 2018, 61, 329–343

ABBREVIATIONS USED

6-AM, 6-acetymorphine; AH, aluminum hydroxide; ALF, Army Liposome Formulation; ALFA, Army Liposome Formulation with aluminum hydroxide; bb, blood−brain; cGLP, current Good Laboratory Practices; cGMP, current Good Manufacturing Practices; IC_{50}, inhibition concentration 50%; IV, intravenous; M-3G, morphine-3-β-glucuronide; M-6G, morphine-6-β-glucuronide; mAb, monoclonal antibody; MPE, maximal potential effect; OMT, opioid management therapy; PBS, Dulbecco's Phosphate Buffered Saline; SC, subcutaneous; SM-$(PEG)_2$, succinimidyl-[(*N*-maleimidopropionamido)-diethylene glycol] ester; TT, tetanus toxoid; TTPT, thermal place preference test

REFERENCES

(1) *Results from the 2013 National Survey on Drug Use and Health: Summary of National Findings*; NSDUH Series H-48, HHS Publication No. (SMA) 14-4863; Substance Abuse and Mental Health Services Administration: Rockville, MD, 2014; pp 1−169.

(2) Center for Behavioral Health Statistics and Quality. *Key Substance Use and Mental Health Indicators in the United States: Results from the 2015 National Survey on Drug Use and Health*; NSDUH Series H-51, HHS Publication No. (SMA) 16-4984; Center for Behavioral Health Statistics and Quality, Substance Abuse and Mental Health Services Administration: Rockville, MD, 2016; pp 1−74.

(3) *QuickStats*: Rates of drug overdose deaths involving heroin, by selected age groups—United States, 2006−2015. *Morb. Mortal. Wkly. Rep.* **2017**, *65*, 1497, DOI 10.15585/mmwr.mm6552a12.

(4) Vocci, F.; Ling, W. Medications development: successes and challenges. *Pharmacol. Ther.* **2005**, *108*, 94−108.

(5) Nielsen, S.; Hillhouse, M.; Mooney, L.; Ang, A.; Ling, W. Buprenorphine pharmacotherapy and behavioral treatment: comparison of outcomes among prescription opioid users, heroin users and combination users. *J. Subst. Abuse Treat.* **2015**, *48*, 70−76.

(6) Jones, J. D.; Sullivan, M. A.; Vosburg, S. K.; Manubay, J. M.; Mogali, S.; Metz, V.; Comer, S. D. Abuse potential of intranasal buprenorphine versus buprenorphine/naloxone in buprenorphine-maintained heroin users. *Addict Biol.* **2015**, *20*, 784−798.

(7) Kosten, T.; Owens, S. M. Immunotherapy for the treatment of drug abuse. *Pharmacol. Ther.* **2005**, *108*, 76−85.

(8) Spector, S.; Berkowitz, B.; Flynn, E. J.; Peskar, B. Antibodies to morphine, barbiturates, and serotonin. *Pharmacol. Rev.* **1973**, *25*, 281−291.

(9) Bremer, P. T.; Kimishima, A.; Schlosburg, J. E.; Zhou, B.; Collins, K. C.; Janda, K. D. Combatting Synthetic Designer Opioids: A conjugate vaccine ablates lethal doses of fentanyl class drugs. *Angew. Chem., Int. Ed.* **2016**, *55*, 3772−3775.

(10) Janda, K. D.; Treweek, J. B. Vaccines targeting drugs of abuse: is the glass half-empty or half-full? *Nat. Rev. Immunol.* **2012**, *12*, 67−72.

(11) Barrett, D. A.; Dyssegaard, A. L.; Shaw, P. N. The effect of temperature and pH on the deacetylation of diamorphine in aqueous solution and in human plasma. *J. Pharm. Pharmacol.* **1992**, *44*, 606−608.

(12) Stowe, G. N.; Schlosburg, J. E.; Vendruscolo, L. F.; Edwards, S.; Misra, K. K.; Schulteis, G.; Zakhari, J. S.; Koob, G. F.; Janda, K. D. Developing a vaccine against multiple psychoactive targets: a case study of heroin. *CNS Neurol. Disord.: Drug Targets* **2011**, *10*, 865−875.

(13) Anton, B.; Leff, P. A novel bivalent morphine/heroin vaccine that prevents relapse to heroin addiction in rodents. *Vaccine* **2006**, *24*, 3232−3240.

(14) Jalah, R.; Torres, O. B.; Mayorov, A. V.; Li, F.; Antoline, J. F.; Jacobson, A. E.; Rice, K. C.; Deschamps, J. R.; Beck, Z.; Alving, C. R.; Matyas, G. R. Efficacy, but not antibody titer or affinity, of a heroin hapten conjugate vaccine correlates with increasing hapten densities on tetanus toxoid, but not on CRM197 carriers. *Bioconjugate Chem.* **2015**, *26*, 1041−1053.

(15) Kosten, T. A.; Shen, X. Y.; O'Malley, P. W.; Kinsey, B. M.; Lykissa, E. D.; Orson, F. M.; Kosten, T. R. A morphine conjugate vaccine attenuates the behavioral effects of morphine in rats. *Prog. Neuro-Psychopharmacol. Biol. Psychiatry* **2013**, *45*, 223−229.

(16) Li, Q. Q.; Luo, Y. X.; Sun, C. Y.; Xue, Y. X.; Zhu, W. L.; Shi, H. S.; Zhai, H. F.; Shi, J.; Lu, L. A morphine/heroin vaccine with new hapten design attenuates behavioral effects in rats. *J. Neurochem.* **2011**, *119*, 1271−1281.

(17) Li, Q. Q.; Sun, C. Y.; Luo, Y. X.; Xue, Y. X.; Meng, S. Q.; Xu, L. Z.; Chen, N.; Deng, J. H.; Zhai, H. F.; Kosten, T. R.; Shi, J.; Lu, L.; Sun, H. Q. A conjugate vaccine attenuates morphine- and heroin-induced behavior in rats. *Int. J. Neuropsychopharmacol.* **2015**, *18*, pyu093.

(18) Matyas, G. R.; Rice, K. C.; Cheng, K.; Li, F.; Antoline, J. F.; Iyer, M. R.; Jacobson, A. E.; Mayorov, A. V.; Beck, Z.; Torres, O. B.; Alving, C. R. Facial recognition of heroin vaccine opiates: type 1 cross-reactivities of antibodies induced by hydrolytically stable haptenic surrogates of heroin, 6-acetylmorphine, and morphine. *Vaccine* **2014**, *32*, 1473−1479.

(19) Raleigh, M. D.; Pravetoni, M.; Harris, A. C.; Birnbaum, A. K.; Pentel, P. R. Selective effects of a morphine conjugate vaccine on heroin and metabolite distribution and heroin-induced behaviors in rats. *J. Pharmacol. Exp. Ther.* **2013**, *344*, 397−406.

(20) Bremer, P. T.; Schlosburg, J. E.; Lively, J. M.; Janda, K. D. Injection route and TLR9 agonist addition significantly impact heroin vaccine efficacy. *Mol. Pharmaceutics* **2014**, *11*, 1075−1080.

(21) Schlosburg, J. E.; Vendruscolo, L. F.; Bremer, P. T.; Lockner, J. W.; Wade, C. L.; Nunes, A. A.; Stowe, G. N.; Edwards, S.; Janda, K. D.; Koob, G. F. Dynamic vaccine blocks relapse to compulsive intake of heroin. *Proc. Natl. Acad. Sci. U. S. A.* **2013**, *110*, 9036−9041.

(22) Stowe, G. N.; Vendruscolo, L. F.; Edwards, S.; Schlosburg, J. E.; Misra, K. K.; Schulteis, G.; Mayorov, A. V.; Zakhari, J. S.; Koob, G. F.; Janda, K. D. A vaccine strategy that induces protective immunity against heroin. *J. Med. Chem.* **2011**, *54*, 5195−5204.

(23) Bremer, P. T.; Schlosburg, J. E.; Banks, M. L.; Steele, F. F.; Zhou, B.; Poklis, J. L.; Janda, K. D. Development of a clinically viable heroin vaccine. *J. Am. Chem. Soc.* **2017**, *139*, 8601−8611.

(24) Li, F.; Cheng, K.; Antoline, J. F.; Iyer, M. R.; Matyas, G. R.; Torres, O. B.; Jalah, R.; Beck, Z.; Alving, C. R.; Parrish, D. A.; Deschamps, J. R.; Jacobson, A. E.; Rice, K. C. Synthesis and immunological effects of heroin vaccines. *Org. Biomol. Chem.* **2014**, *12*, 7211−7232.

(25) Torres, O. B.; Matyas, G. R.; Rao, M.; Peachman, K. K.; Jalah, R.; Beck, Z.; Michael, N. L.; Rice, K. C.; Jacobson, A. E.; Alving, C. R. Heroin-HIV-1 (H2) vaccine: induction of dual immunologic effects with a heroin hapten-conjugate and an HIV-1 envelope V2 peptide with liposomal lipid A as an adjuvant. *npj Vaccines* **2017**, *2*, 13.

(26) *Drugs of Abuse, A DEA Resource Guide*: 2017 ed.; Penny Hill Press, 2017; https://go.usa.gov/xN7Qm.

(27) Olofson, R. A.; Martz, J. T.; Senet, J. P.; Piteau, M.; Malfroot, T. A new reagent for the selective, high-yield *N*-dealkylation of tertiary amines: improved syntheses of naltrexone and nalbuphine. *J. Org. Chem.* **1984**, *49*, 2081−2082.

(28) Jung, M. E.; Lyster, M. A. Conversion of alkyl carbamates into amines via treatment with trimethylsilyl iodide. *J. Chem. Soc., Chem. Commun.* **1978**, 315−316.

(29) Kosugi, M.; Kameyama, M.; Migita, T. Palladium-catalyzed aromatic amination of aryl bromides with *N,N*-dimethylaminotributyltin. *Chem. Lett.* **1983**, *12*, 927−928.

(30) Surry, D. S.; Buchwald, S. L. Dialkylbiaryl phosphines in Pd-catalyzed amination: A user's guide. *Chem. Sci.* **2011**, *2*, 27−50.

(31) Evano, G.; Blanchard, N.; Toumi, M. Copper-mediated coupling reactions and their applications in natural products and designed biomolecules synthesis. *Chem. Rev.* **2008**, *108*, 3054−3131.

(32) Bruno, N. C.; Buchwald, S. L. Synthesis and application of palladium precatalysts that accommodate extremely bulky di-tert-butylphosphino biaryl ligands. *Org. Lett.* **2013**, *15*, 2876−2879.

DOI: 10.1021/acs.jmedchem.7b01427
J. Med. Chem. 2018, 61, 329−343

(33) Hicks, J. D.; Hyde, A. M.; Cuezva, A. M.; Buchwald, S. L. Pd-catalyzed *N*-arylation of secondary acyclic amides: catalyst development, scope, and computational study. *J. Am. Chem. Soc.* **2009**, *131*, 16720−16734.
(34) Hudson, J. A.; Sweeney, J. B. An efficient method for reductive amination of carbonyl compounds under nonacidic conditions. *Synlett* **2012**, *23*, 2176−2178.
(35) Miriyala, B.; Bhattacharyya, S.; Williamson, J. S. Chemoselective reductive alkylation of ammonia with carbonyl compounds: synthesis of primary and symmetrical secondary amines. *Tetrahedron* **2004**, *60*, 1463−1471.
(36) Temperini, A.; Terlizzi, R.; Testaferri, L.; Tiecco, M. Additive-fee chemoselective acylation of amines. *Synth. Commun.* **2009**, *40*, 295−302.
(37) González-Sabín, J.; Gotor, V.; Rebolledo, F. CAL-B-catalyzed resolution of some pharmacologically interesting β-substituted isopropylamines. *Tetrahedron: Asymmetry* **2002**, *13*, 1315−1320.
(38) Beck, Z.; Matyas, G. R.; Jalah, R.; Rao, M.; Polonis, V. R.; Alving, C. R. Differential immune responses to HIV-1 envelope protein induced by liposomal adjuvant formulations containing monophosphoryl lipid A with or without QS21. *Vaccine* **2015**, *33*, 5578−5587.
(39) Torres, O. B.; Antoline, J. F.; Li, F.; Jalah, R.; Jacobson, A. E.; Rice, K. C.; Alving, C. R.; Matyas, G. R. A simple nonradioactive method for the determination of the binding affinities of antibodies induced by hapten bioconjugates for drugs of abuse. *Anal. Bioanal. Chem.* **2016**, *408*, 1191−204.
(40) Alving, C. R.; Matyas, G. R.; Torres, O.; Jalah, R.; Beck, Z. Adjuvants for vaccines to drugs of abuse and addiction. *Vaccine* **2014**, *32*, 5382−5389.
(41) Knuf, M.; Kowalzik, F.; Kieninger, D. Comparative effects of carrier proteins on vaccine-induced immune response. *Vaccine* **2011**, *29*, 4881−4890.
(42) Rao, M.; Alving, C. R. Adjuvants for HIV vaccines. *Curr. Opin. HIV AIDS* **2016**, *11*, 585−592.
(43) Alving, C. R.; Beck, Z.; Matyas, G. R.; Rao, M. Liposomal adjuvants for human vaccines. *Expert Opin. Drug Delivery* **2016**, *13*, 807−816.
(44) Alving, C. R.; Rao, M.; Steers, N. J.; Matyas, G. R.; Mayorov, A. V. Liposomes containing lipid A: an effective, safe, generic adjuvant system for synthetic vaccines. *Expert Rev. Vaccines* **2012**, *11*, 733−744.
(45) Matyas, G. R.; Mayorov, A. V.; Rice, K. C.; Jacobson, A. E.; Cheng, K.; Iyer, M. R.; Li, F.; Beck, Z.; Janda, K. D.; Alving, C. R. Liposomes containing monophosphoryl lipid A: a potent adjuvant system for inducing antibodies to heroin hapten analogs. *Vaccine* **2013**, *31*, 2804−2810.
(46) Matyas, G. R.; Muderhwa, J. M.; Alving, C. R. Oil-in-water liposomal emulsions for vaccine delivery. *Methods Enzymol.* **2003**, *373*, 34−50.
(47) Gable, R. S. Comparison of acute lethal toxicity of commonly abused psychoactive substances. *Addiction* **2004**, *99*, 686−696.
(48) Lee, M. Y.; Shin, M. C.; Yang, V. C. Transcutaneous antigen delivery system. *BMB Rep* **2013**, *46*, 17−24.
(49) Andersen, J. M.; Ripel, A.; Boix, F.; Normann, P. T.; Morland, J. Increased locomotor activity induced by heroin in mice: pharmacokinetic demonstration of heroin acting as a prodrug for the mediator 6-monoacetylmorphine in vivo. *J. Pharmacol. Exp. Ther.* **2009**, *331*, 153−161.
(50) Compton, W. M.; Jones, C. M.; Baldwin, G. T. Relationship between nonmedical prescription-opioid use and heroin use. *N. Engl. J. Med.* **2016**, *374*, 154−163.
(51) Kolodny, A.; Courtwright, D. T.; Hwang, C. S.; Kreiner, P.; Eadie, J. L.; Clark, T. W.; Alexander, G. C. The prescription opioid and heroin crisis: a public health approach to an epidemic of addiction. *Annu. Rev. Public Health* **2015**, *36*, 559−574.
(52) Volkow, N. D.; McLellan, A. T. Opioid abuse in chronic pain−misconceptions and mitigation strategies. *N. Engl. J. Med.* **2016**, *374*, 1253−1263.
(53) Pravetoni, M.; Raleigh, M. D.; Le Naour, M.; Tucker, A. M.; Harmon, T. M.; Jones, J. M.; Birnbaum, A. K.; Portoghese, P. S.; Pentel, P. R. Co-administration of morphine and oxycodone vaccines reduces the distribution of 6-monoacetylmorphine and oxycodone to brain in rats. *Vaccine* **2012**, *30*, 4617−4624.
(54) Pravetoni, M.; Le Naour, M.; Tucker, A. M.; Harmon, T. M.; Hawley, T. M.; Portoghese, P. S.; Pentel, P. R. Reduced antinociception of opioids in rats and mice by vaccination with immunogens containing oxycodone and hydrocodone haptens. *J. Med. Chem.* **2013**, *56*, 915−923.
(55) Torres, O. B.; Jalah, R.; Rice, K. C.; Li, F.; Antoline, J. F.; Iyer, M. R.; Jacobson, A. E.; Boutaghou, M. N.; Alving, C. R.; Matyas, G. R. Characterization and optimization of heroin hapten-BSA conjugates: method development for the synthesis of reproducible hapten-based vaccines. *Anal. Bioanal. Chem.* **2014**, *406*, 5927−5937.
(56) Bannon, A. W.; Malmberg, A. B. Models of nociception: hot-plate, tail-flick, and formalin tests in rodents. In *Current Protocols in Neuroscience*; Wiley: New York, 2007; Chapter 8, unit 8.09, DOI 10.1002/0471142301.ns0809s41.
(57) Le Bars, D.; Gozariu, M.; Cadden, S. W. Animal models of nociception. *Pharmacol. Rev.* **2001**, *53*, 597−652.
(58) Balayssac, D.; Ling, B.; Ferrier, J.; Pereira, B.; Eschalier, A.; Authier, N. Assessment of thermal sensitivity in rats using the thermal place preference test: description and application in the study of oxaliplatin-induced acute thermal hypersensitivity and inflammatory pain models. *Behav. Pharmacol.* **2014**, *25*, 99−111.

DOI: 10.1021/acs.jmedchem.7b01427
J. Med. Chem. 2018, 61, 329−343